which is coencapsulated in the vesicles (*27*, *28*). As a result, the functional half-life of the Hb-vesicles is doubled by coencapsulation of the DL-homocysteine and active oxygen scavengers (*27*, *29*). To retard metHb formation, bioconjugation of enzymes such as catalase or superoxide dismutase (SOD) (*30*) and coencapsulation of RBC enzymes including the metHb reductase system, carbonic anhydrase, SOD, or catalase (*29*, *31*) have also been reported.

To restore the O_2 binding property of HbV, we tested utilization of the photoreduction system: the indirect excitation of an externally added electron mediator (*32*), or the direct excitation of metHb absorption in the UV region (*7*). In this study, we have made significant efforts to find out a condition that facilitates metHb reduction by a photoreduced flavin mononucleotide (FMN), because this system was well characterized by Everse (*32*), and the advantages of this system are visible light irradiation and high quantum yield (*9*, *10*). We analyzed the influence of electron donors to FMN, dissolved gases, etc., to find the facilitating condition and elucidate the mechanism for the facilitation of the metHb photoreduction in the HbV nanoparticles, a structure similar to that in red blood cells (RBCs), and this may also help understand the underlying mechanism of the reaction of NADPH-flavin reductase and metHb in RBCs.

EXPERIMENTAL PROCEDURES

Preparation of metHb. Carbonylhemoglobin (HbCO) was purified from outdated donated blood offered by the Hokkaido Red Cross Blood Center as previously reported (*33*, *34*). MetHb was prepared by reacting HbCO with an excess amount of potassium ferricyanide. The unreacted ions and ferrocyanide ions were removed twice by stirring with a mixed bed ion-exchange resin (Bio Rad AG 501-X8), and the solution was then permeated through 0.22 μm-filters (Advantec Co.). The metHb conversion was 99.8% measured by the cyanomethemoglobin method.

Chemicals. Amino acids (Met, Gln, Arg, Glu, Phe, Lys, Tyr, and Trp) were purchased from the Kanto Chem. Co (Tokyo). Peptides (Met-Met and Met-Gly) were from Sigma, and saccharides (mannitol, maltotriose, dextran, glucoseamine, glucron amide), methanol, citric acid sodium salt, ethylenediamine tetraacetic acid (EDTA), and diethylenetriamine pentaacetic acid (DTPA) were from the Kanto Chem. Co. All the chemicals were used without purification.

Photoreduction of FMN in the Presence of an Electron Donor. Three milliliters of phosphate-buffered saline (10 mM PBS, pH 7.4) with an electron donor (e.g., amino acids, peptides, sugars, as listed above, 20 mM) was sealed in a cuvette (2 mm width) with a butyl rubber cap. The solution was bubbled with N_2 for 30 min. A stock solution of FMN prepared in the dark was added at a concentration of 10 μM. The light source was a super high-pressure mercury lamp (USH-250D, 250W, Ushio Co., Tokyo) with a cutoff filter (L-42 and HA-50, Hoya Co., Tokyo) to obtain a single beam with the maximum wavelength of about 435 nm, which is close to λ_{max} of FMN (450 nm). The cuvette was located 2.5 cm away from the light source, and the light intensity was 221 mW/cm^2 that was measured with a power meter (PSV-3102, Gentec Co.). The conversion of the reduction, FMN to $FMNH_2$, was calculated from the reduction of absorbance at 450 nm, measured with an UV/vis spectrophotometer (V-560, Jasco, Tokyo).

Photoreduction of metHb in the Presence of FMN and an Electron Donor. Three milliliters of phosphate-buffered saline (10 mM PBS, pH 7.4) with an electron donor and FMN was sealed in a cuvette (2 mm width) with a butyl rubber cap. The solution was bubbled with N_2 gas for 30 min. A concentrated metHb stock solution deaerated by a gentle N_2 flowing in another bottle (about 3 mM, 10 μL) was injected into the cuvette. This procedure avoided bubbling of a metHb solution that might induce foaming and metHb denaturation. The final concentration of heme was 0.1 mM. The cuvette was exposed to the same visible light (435 nm) as described above. The conversion of the metHb reduction was calculated from the ratio of the Soret band absorption at 405 nm (λ_{max} of metHb) versus 430 nm (deoxyHb) or 415 nm (HbO_2).

A laser flash photolysis system (Tokyo Instr. Co.) was used for the transient spectrum measurement of the reduction of FMN and the succeeding metHb (*7*). The sample solutions were excited at 450 nm with a Pulsed Nd:YAG laser (SL803G-10, Spectron Laser Systems, Ltd.) equipped with an optical parametric oscillator. One irradiation time was 5–8 ns (fwhm) and the interval was 100 ms. A total of 100 accumulations were collected to get an acceptable signal-to-noise ratio. The transient spectra were recorded between 350 and 550 nm using a spectrophotometer (MS257, Oliel Instr. Co.) equipped with an ICCD detector (DH520–18F–WR, ANDOR Technol. Co.). A sample solution was placed in a 10 mm quartz cuvette and purged with N_2. The fastest time point of the measurements was 30 ns. A solution of FMN (100 μM)/Met (20 mM) in a 10 mM phosphate-buffered saline (pH 7.4), and a solution of FMN (5 μM)/Met (20 mM)/metHb ([heme] = 10 μM) in the phosphate-buffered saline were tested.

Quantum Yield Measurement. The ferroioxalate actinometer of $K_3[Fe(C_2O_4)_3]\cdot 3H_2O$ was used to measure the quantum yield (Φ) of metHb photoreduction (*7*, *35*, *36*). In the actinometer, Φ of the photoreduction of Fe^{3+} to Fe^{2+} was assumed to be 1.11 (*35*), and this value was used to calculate the total photons absorbed by the sample solution and Φ of the metHb photoreductions.

Isoelectric Focusing (IEF) and Native Polyacrylaminde Gel Electrophoresis (Native-PAGE). IEF and native-PAGE were performed on PhastGel IEF 3–9 (pH 3–9) and PhastGel Gradient 8–25 (PAGE content, 8–25%) (Amersham Pharmacia Biotech), respectively, with the PhastSystem (Pharmacia). The photoreduced Hbs in N_2 and air in the presence of FMN/EDTA was compared with metHb and the purified HbO_2.

IEF. Forty microliters of sample (1 mg/mL) per one lane was applied on the gel. This was focused and then stained with PhastGel Blue R (Coomassie brilliant blue) in the development unit of the PhastSystem. The marker was the p*I* calibration kit 3–10 (Pharmacia).

Native-PAGE. The samples were applied on the gel and the electrophoresis was automatically performed. The gel was stained with PhastGel Blue R. The marker was HMW Kit E (Parmacia).

Restoration of Oxygen Binding Property. The photoreduced deoxyHb solution ([heme] = 20 mM, [FMN] = 5 μM, [EDTA] = 10 mM) in an Ar atmosphere was bubbled with oxygen, and the UV/vis spectroscopy was measured. The photoreduced Hb solution was permeated through a column of Sephadex G-25 (Pharmacia) to remove FMN, the oxygen equilibrium curve of the obtained Hb solution was obtained at 37 °C with a Hemox Analyzer (TCS Products Inc.), and the oxygen affinity (P_{50}) and Hill number were measured. The Hb samples were diluted in a Hemox phosphate buffer (TCS Products Inc.).

Preparation of Hb-Vesicles Coencapsulating FMN and EDTA, and the Photoreduction of metHb. HbVs were prepared as previously reported (*24*, *34*, *37*). The purified HbO_2 solution (35 g/dL, [heme] = 21.7 mM) contained FMN (5, 10, or 50 mM) and EDTA (10, 20, 30, 50, or 200 mM), this was mixed with the lipid mixtures, and the resulting multilamellar vesicles were extruded through filters to regulate the vesicular size. The lipid bilayer was composed of a mixture of 1,2-dipalmitoyl-*sn*-glycero-3-phosphatidylcholine (DPPC), cholesterol, and 1,5-*O*-dihexadecyl-*N*-succinyl-L-glutamate (DHSG) at the molar ratio of 5/5/1 (Nippon Fine Chem. Co., Osaka), and 1,2-distearoyl-*sn*-glycero-3-phosphatidylethanolamine-*N*-PEG_{5000} (PEG-DSPE, NOF Co., Tokyo) (*38*). Thus the vesicular surface was covered with PEG chains. The molar composition of the DPPC/cholesterol/DHSG/PEG-DSPE was 5/5/1/0.033. HbVs were suspended in a physiologic salt solution at [Hb] = 10 g/dL. The suspension was incubated in the dark at 40 °C for 48 h to facilitate the metHb formation and to prepare metHbV. The concentrations of FMN, EDTA, and heme of Hb in HbV, expressed as $[FMN]_{in}$, $[EDTA]_{in}$, and $[heme]_{in}$, respectively, are assumed to be identical to the fed concentrations for the HbV preparation.

Photoreduction of metHbV was performed in the same manner with a metHb solution in a relatively diluted condition ([heme] = 10 μM) in a 2 mm quartz cuvette. At a higher concentration ([heme] = 5 mM) under aerobic condition, the suspension of metHbV was sandwiched between two glass plates. The optical path length was 10 μm.

Measurement of H_2O_2 in the metHb Photoreduction. The reaction of *p*-hydroxyphenyl acetic acid (PHA) and H_2O_2 to generate a fluorescent dimer, 6,6′-dihydroxy (1,1′-biphenyl)-3,3′-diacetic acid (DBDA), was used to detect H_2O_2 generated during the metHb photoreduction in the metHbV and metHb solutions. During the photoreduction of metHb or metHbV ([heme] = 20 μM in a cuvette) in the presence of FMN (5 μM)/EDTA (50 μM), 1 mL of sample was pipetted out and immediately mixed with horseradish peroxidase (Sigma, 3.7 μM), and PHA (5.8 mM). The mixture was ultracentrifuged in a tube with a filter (Cut off Mw. 30 kDa, Ultrafree, Amicon) at 12 000 rpm for 20 min to remove Hb or HbV and to obtain the filtrate solution. The fluorescence of the filtrate was measured with a fluorometer (JASCO, Ex: 317 nm, Em: 404 nm). The calibration curve was obtained by analysis of a diluted standard H_2O_2 solution (Kanto Chem., Co).

RESULTS

Photoreduction of FMN with an Electron Donor. Figure 1 shows the time course of the conversion of FMN to $FMNH_2$ by irradiation of visible light (435 nm). FMN primarily converts to the photoexcited triplet FMN* and this reacts with two electron donors (D) to generate $FMNH_2$. The reduction can be confirmed by the decrease in the absorption of the characteristics peaks at 370 and 450 nm. Without an addition of an electron donor, photoreduction gradually proceeds (baseline, initial reduction rate = 12 μM/min) (Table 1). A ribityl group in a FMN molecule of itself can be an electron donor. However, further irradiation should induce decomposition that was evident from the phenomena that the spectroscopic curves did not coincide at the isosbestic point. A significantly fast reduction was observed by the addition of EDTA and DTPA that were 88 and 84 times faster than the condition without the addition of an electron donor. Among the amino acids, Met showed the fastest

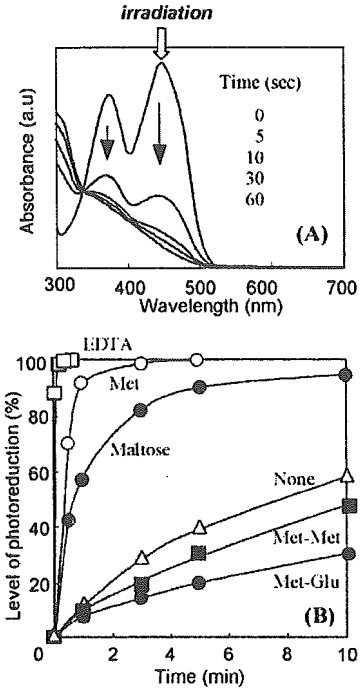

Figure 1. (A) Time course of the spectral changes during the conversion of FMN to $FMNH_2$ in the presence of EDTA (20 mM) by visible light irradiation (435 nm). The characteristic two peaks disappeared with the photoreduction conversion. (B) Time course of the conversion of FMN to $FMNH_2$ with various electron donors. EDTA and Met showed fast photoreduction rate. On the other hand, Met-Met and Met-Glu retarded the reaction. [FMN] = 100 μM, [electron donor] = 20 mM, pH = 7.4, in N_2 atmosphere.

Table 1. Initial Rates of the Photoreduction of FMN to $FMNH_2$ with Various Electron Donors (10 mM)

electron donor	mw	initial reduction rate (μM/min)	comparison with baseline
EDTA	292	1056	88
DTPA	393	1008	84
Met	149	140	11.7
Met-Met (10 mM)	280	5	0.2
Met-Met (20 mM)	280	10	0.8
Met-Glu	278	7	0.6
Arg	174	124	10.3
Phe	165	118	9.8
Lys	146	104	8.7
Gln	146	58	4.8
Glu	147	46	3.8
mannitol	182	45	3.8
maltotriose (10 unit mM)	504	47	3.9
dextran (10 unit mM)	5×10^6	45	3.6
glucoseamine	216	100	8.3
glucron amide	193	72	6.0
methanol	32	42	3.5
citric acid sodium salt	294	40	3.3
hydrogen	2	82	6.8
none (baseline)	- - -	12	1.0

reduction rate (140 μM/min, 12 times faster than the baseline), while Arg, Phe, Lys, Glu, and Gln showed moderate facilitation. On the other hand, Tyr and Trp showed slower rates of photoreduction. Unexpectedly, Met-Met and Met-Glu lowered the reduction rate. As for the saccharides, mannitol, maltotriose, dextran, glucosamine, and glucron amide showed similar facilitation at the same glucose units. However, they are much slower than Met and EDTA. The presence of H_2 gas

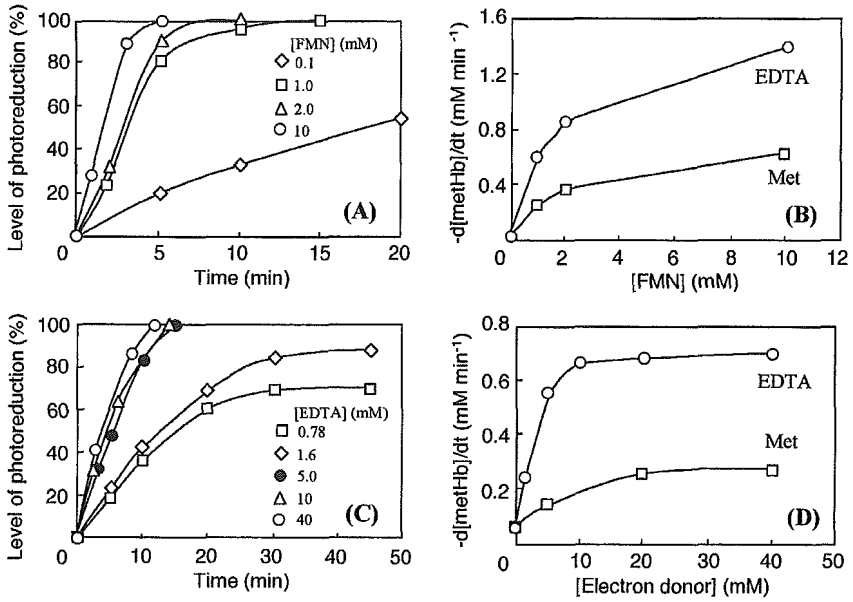

Figure 2. Influence of the concentrations of FMN and EDTA on the rate of metHb reduction. The time course of the level of photoreduction and the initial reaction rates are summarized. (A, B): Influence of the FMN concentration at a constant [EDTA] (20 mM). [FMN] was at 0.1, 1.0, 2.0, or 10 mM. (C, D): Influence of [EDTA] at the constant [FMN] (1.0 mM). [EDTA] was at 0.78, 1.6, 5.0, 10, or 40 mM. The data for the Met addition were inserted as a reference. [heme] = 3.1 mM.

slightly facilitated the reduction. Citric acid and methanol showed a slight facilitation. From these results, EDTA and Met were mainly studied as electron donors.

Reduction of metHb by the Photoreduced FMNH$_2$. The reduction of metHb by the photoreduced $FMNH_2$ was evident from the spectroscopic change of λ_{max} in the Soret and Q-bands. The influence of the concentration of FMN was examined at constant concentrations of metHb (5 g/dL, [heme] = 3.1 mM) and EDTA (20 mM) (Figure 2A). The presence of 100 μM FMN showed 50% reduction of metHb at 20 min; however, 1 mM FMN completed the reduction at 15 min. The influence of the EDTA concentration was examined at constant concentrations of metHb ([heme] = 3.1 mM) and FMN (1.0 mM) (Figure 2B). Without EDTA, the metHb photoreduction proceeded since a ribityl group of FMN and probably globin of Hb can be an electron donor. When the EDTA concentration was less than that of the heme concentration, the reduction rate was very slow, and the reduction could not be completed. However, 5 mM EDTA and higher showed a faster rate and the reduction was completed within 15 min. Similar results were obtained with Met; however, the initial rates were much slower than with EDTA.

The transient spectrum of the photoreduction of FMN in the presence of Met after laser flash irradiation showed the reduction of the absorbances at 445 and 373 nm at 30 ns, and the spectral profile was the same at 5 ms (data not shown here). Therefore, the photoreduction of FMN to $FMNH_2$ was completed within 30 ns. In the presence of metHb, a total of 30 ns was enough to observe the reduced deoxyHb (λ_{max} = 430 nm) and the spectrum was the same for 5 ms.

The influence of the presence of O_2 was examined (Figure 3). The metHb photoreduction in the presence of EDTA and FMN in the N_2 atmosphere completed the reduction within 15 min. The metHb photoreduction under the aerobic conditions became slightly slower, and the level of reduction reached 95% and then showed a plateau. In the case of the addition of Met, the reduction was completed within 40 min in the N_2 atmosphere that

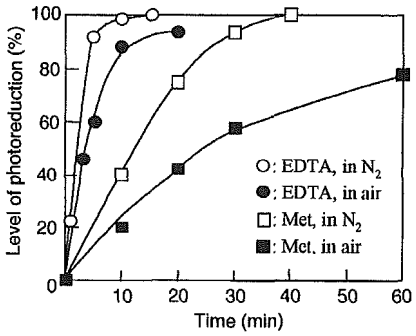

Figure 3. The influence of the presence of O_2 on the rate of photoreduction of metHb ([heme] = 3.1 mM) with FMN (1.0 mM) and an electron donor (20 mM) at pH 7.4. The data for Met addition (1.0 mM) were also inserted as a reference. The presence of O_2 retarded the metHb photoreduction.

was much slower in comparison with the EDTA addition. Under the aerobic condition, the reduction in the presence of Met was significantly slow and did not reach 80% at 60 min.

Native-PAGE of the photoreduced Hb both in the N_2 and aerobic atmospheres showed identical bands with the normal oxyHb and meHb (Figure 4A). Even though the Mw of Hb is 64.5 kDa, it showed a higher relative Mw than albumin (67 kDa) as one of the markers in the Native-PAGE in the absence of sodium dodecyl sulfate, SDS, because the surface charge of the protein directly affect on the traveling distance during the electrophoresis. IEF of the photoreduced Hbs showed the presence of HbO_2 at pI = 7.0 as a dense band and a weak band at pI = 7.2 of a partially reduced Hb (Figure 4B). There was no band at 7.4 that corresponds to metHb.

The oxygen dissociation curve of the photoreduced Hb was identical with that of the normal HbO_2 (Data not shown here). The P_{50} and Hill number of the photoreduced Hb were 10.5 Torr and 1.8, respectively, and they were almost identical with the normal HbO_2 (11 Torr and 1.7, respectively).

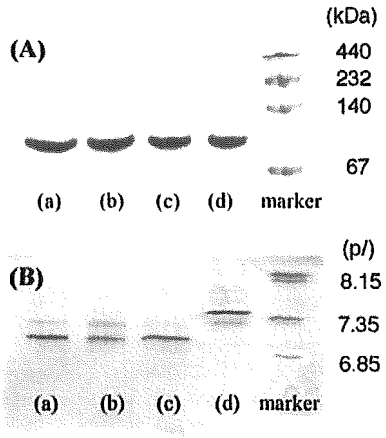

Figure 4. Native-PAGE (A) and IEF (B) of the photoreduced Hb in the presence of EDTA and FMN both in N_2 and aerobic atmospheres: (a) photoreduced Hb in N_2, (b) photoreduced Hb in air, (c) oxyHb, (d) metHb. In A, there was no change in the molecular weight of the Hb subunits. Since Native-PAGE does not include sodium dodecyl sulfate, the surface property of the protein directly affect on the traveling distance during electrophoresis. Therefore, Mw of Hb (Mw = 64.5 kDa) seemed much larger than albumin marker (Mw = 67 kDa). In B, the band at 7.4, which corresponded to metHb, almost disappeared in lanes a and b. No other bands were observed.

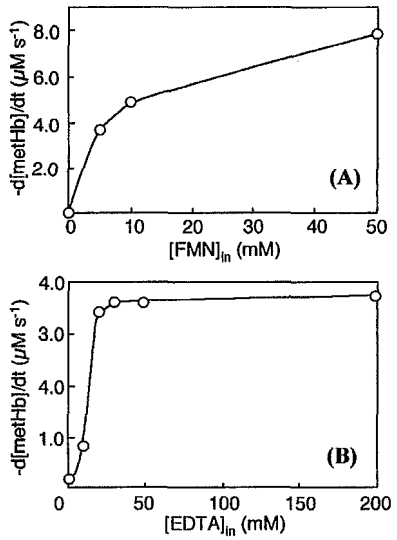

Figure 5. Influence of the concentrations of FMN and EDTA inside HbV on the initial rate of metHb reduction. (A) Influence of $[FMN]_{in}$ at the constant $[EDTA]_{in}$ = 20 mM. (B) Influence of $[EDTA]_{in}$ at the constant $[FMN]_{in}$ = 5 mM. [heme] = 10 μM in the cuvette, $[heme]_{in}$ = 21.7 mM. When $[EDTA]_{in}$ was higher than $[heme]_{in}$, the initial rate of metHb reduction was plateau.

Reduction of metHb in Hb-Vesicles. At first a diluted metHbV suspension ([heme] = 10 μM in a cuvette; $[heme]_{in}$ = 21.7 mM) was tested for photoreduction to analyze the kinetics. The initial rate of metHb reduction increased with increasing $[FMN]_{in}$ at a constant $[EDTA]_{in}$ (20 mM); however, the initial rate at $[FMN]_{in}$ = 10 mM was lower than twice that at $[FMN]_{in}$ = 5 mM (Figure 5A). At a constant $[FMN]_{in}$ (5 mM), increasing the $[EDTA]_{in}$ significantly facilitated the metHb photoreduction, however, the photoreduction rate did not increase above 20 mM (Figure 5B). This critical concentration is almost identical to $[heme]_{in}$ (21.7 mM). From these results, the rate-determining step of this system should be the electron transfer from an electron donor to the photoexcited FMN.

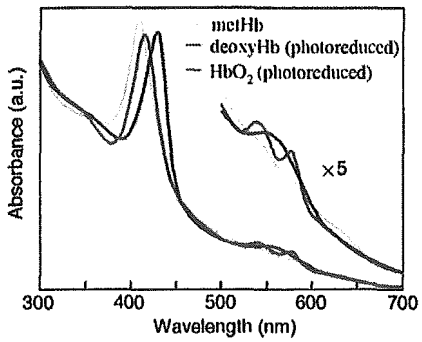

Figure 6. UV–visible spectra of HbV before irradiation (metHb), after photoreduction (deoxyHb), and its oxygenated form (HbO_2). $[EDTA]_{in}$ = 50 mM, $[FMN]_{in}$ = 5 mM, $[heme]_{in}$ = 21.7 mM. These spectra indicate the successful restoration of O_2-binding property of HbV.

The absorption spectra of the metHbV and the photoreduced HbV (λ_{max} = 430 nm) are shown in Figure 6. Due to the light scattering effect of the HbV particles, the turbidity was higher at a lower wavelength (*39*). Bubbling with an O_2 gas in a photoreduced HbV solution reversibly converted deoxyHb to HbO_2 with a characteristic shift of λ_{max} from 430 to 415 nm, indicating that the oxygen binding ability was successfully restored.

The concentration of [heme] in an HbV suspension for the intravenous infusion should be estimated to about 3–6 mM, which is significantly higher in comparison with 10 μM in a cuvette for the absorption spectral analysis. To test the photoreduction at a practical Hb concentration, a metHbV suspension ([heme] = 5.0 mM) was sandwiched between two glass plates and irradiated with visible light. The photoreduction proceeded quite promptly (Figure 7). Due to the thin liquid layer (ca. 10 μm in thickness), the effect of light scattering seen in Figure 6 is minimized. At the constant $[FMN]_{in}$ (5 mM) condition, the $[EDTA]_{in}$ of 10 and 20 mM were not enough to complete the reduction. At $[EDTA]_{in}$ = 50 mM, the photoreduction was significantly fast and the reaction was completed within 20 s with the characteristic λ_{max} of deoxyHb (430 nm). At $[FMN]_{in}$ = 100 mM and $[EDTA]_{in}$ = 20 mM, the initial reduction rate was the fastest; however, the reduction was not completed which was evident from the fact that the absorption at 430 nm in the Soret band was not high enough. The value of $[EDTA]_{in}$ should at least be higher than $[heme]_{in}$ (21.7 mM).

Quantum Yield of the Photoreduction Reactions. Table 2 summarizes the quantum yield, Φ, of various photoreduction conditions. The combination of metHb/FMN/EDTA showed the highest value (0.17) in an Ar atmosphere at [heme] = 0.1 mM. This was about 28 times higher than that for the photoreduction by the direct excitation of the N-band irradiating by near UV light (365 nm, Φ = 0.003–0.006) (*7*), and 4 times higher than the condition without an electron donor (0.04). In the case of HbV that coencapsulates FMN and EDTA, the concentrations of the components in the cuvette were much smaller, however, the concentrations in the nanoparticles (HbV) are much higher and the Φ for HbV was also very high (0.09–0.11). Probably due to the light scattering effect of HbV, Φ for HbV is slightly lower than that for the homogeneous Hb solution, but significantly higher than that for the N-band excitation (0.003–0.006).

Measurement of H_2O_2 in the metHb Photoreduction. Visible light irradiation to metHb([heme] = 20 μM)/FMN(5 μM)/EDTA(50 μM) under aerobic conditions

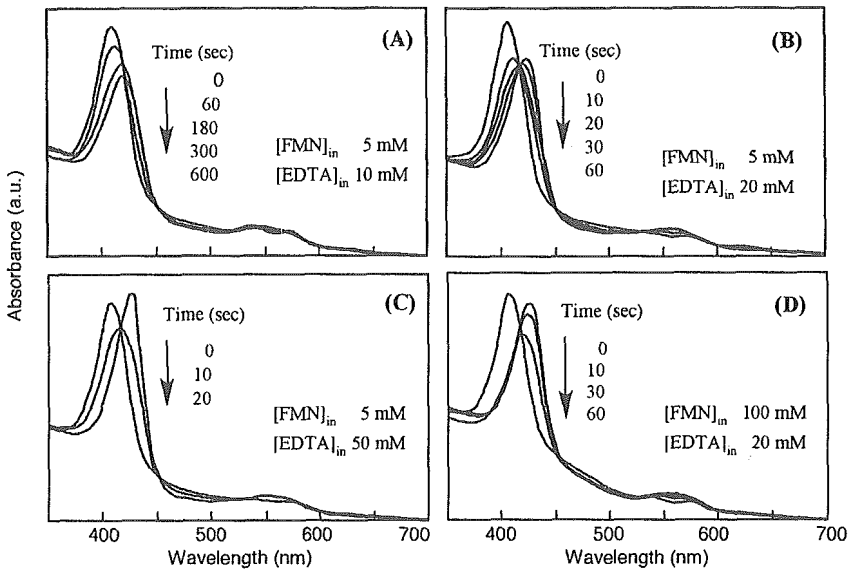

Figure 7. UV–visible spectral changes of HbV in a liquid layer sandwiched between two glass plates during photoreduction under aerobic conditions. The thickness of the layer was approximately 10 μm. Condition (C) ($[FMN]_{in}$ = 5 mM, $[EDTA]_{in}$ = 50 mM) showed the fastest rate of photoreduction, and the reaction was completed within 20 s. The arrows indicate the decrease in absorbance at 405 nm of MetHb with irradiation time.

Table 2. Quantum Yield (Φ) of Photoreduction of metHb and metHbV

	heme (mM)	FMN (mM)	electron donor (mM)	condition	λ_{ex} (nm)	Φ
metHb	0.1	0.01	EDTA (20)	in Ar	435	0.17
	0.1	0.01	Met (20)	in Ar	435	0.11
	0.1	0.01	no addition	in Ar	435	0.04
metHbV	0.01 (21.7)[a]	2.3×10^{-3} (5)[a]	EDTA (9.2×10^{-3}) (20)[a]	in Ar	435	0.09
	0.01 (21.7)[a]	46×10^{-3} (100)[a]	EDTA (9.2×10^{-3}) (20)[a]	in Ar	435	0.11
metHb	0.01	–	Trp (1.0)	in Ar	365	0.006[b]
	0.01	–	mannitol (100)	in CO	365	0.006[b]
	0.01	–	no addition	in CO	365	0.003[b]

[a] Concentrations of the components inside HbV; $[heme]_{in}$, $[FMN]_{in}$, $[EDTA]_{in}$. [b] Data from ref 7.

produced H_2O_2, and the fluorescent intensity of DBDA (λ_{em} = 404 nm) significantly increased (Figure 8a). The amount of H_2O_2 reached 40 μM at 120 s (Figure 8b). Irradiation to FMN alone produced 100 μM H_2O_2 for 120 s without any formation of $FMNH_2$. We confirmed that the irradiation to metHb alone did not produce H_2O_2 (data not shown here). The level of metHb photoreduction was less than 20% at 120 s (Figure 8c). A significant suppression of H_2O_2 generation was confirmed for the irradiation to metHbV and the H_2O_2 generation decreased to less than 20 μM, and the level of metHb photoreduction reached 50% at 120 s. A further increase in the level of photoreduction to 80% was confirmed when the partial oxygen pressure in the cuvette was regulated to 40 Torr; however, the amount of H_2O_2 could not be significantly reduced.

DISCUSSION

We found for the first time that the coencapsulation of concentrated Hb solution and the FMN/EDTA system in phospholipid vesicles (HbV) significantly facilitated the reduction of metHb by visible light irradiation (435 nm). This was evident from the Φ of the reaction, i.e., 0.17 for the Hb solution and 0.10 for the HbV suspension. The lowered Φ for HbV in comparison with that for a Hb solution is probably due to the light scattering of the illuminated visible light due to the particle of HbV (diameter, 250 nm) (*39*). However, they are much higher than that for the metHb photoreduction via direct photoexcitation of the N-band of the porphyrin ring in the UVA region (Φ = 0.006) (*7*). Even though the concentrations of the components in the cuvette were much lower for HbV than for the homogeneous Hb solution as shown in Table 2, the concentrations inside HbV were significantly higher and this condition facilitated the desired reactions (photoreduction of FMN and metHb) and suppressed the unwanted side reactions (generation of active oxygen species).

The reaction mechanism is that the photoexcited triplet FMN* rapidly receives an electron from the donor molecule, EDTA, to transform to the semiquinone followed by disproportionation to the two electron reduced form, $FMNH_2$. They are effective reducing agent to offer an electron to metHb. According to Yubisui et al., $FMNH_2$ reduces metHb with the rate constant of 5.5×10^6 M^{-1} s^{-1} (*22*), which is significantly faster than do glutathione (rate constant = 2.5×10^{-3} M^{-1} s^{-1}) (*27*) and ascorbic acid (3.0×10^{-3} M^{-1} s^{-1}) (*22*). The transient spectrum of the reduction of metHb by the photoreduced form of FMN demonstrated the completion of the reaction at 30 ns. Our result may be plausible because it is reported that a flavocytochrome showed complete photoreduction within 100 ns (*14*), measured by a laser flash-induced transient absorption difference spectra. The externally added FMN should more freely access to the protoporphyrin IX (heme) in the Hb molecule and would show a faster electron transfer. It is reported that the direct chemical conjugation of flavin to the propionic acid residue of heme significantly facilitates the electron transfer from flavin to heme in a reconstituted myoglobin (*40*, *41*). Therefore,

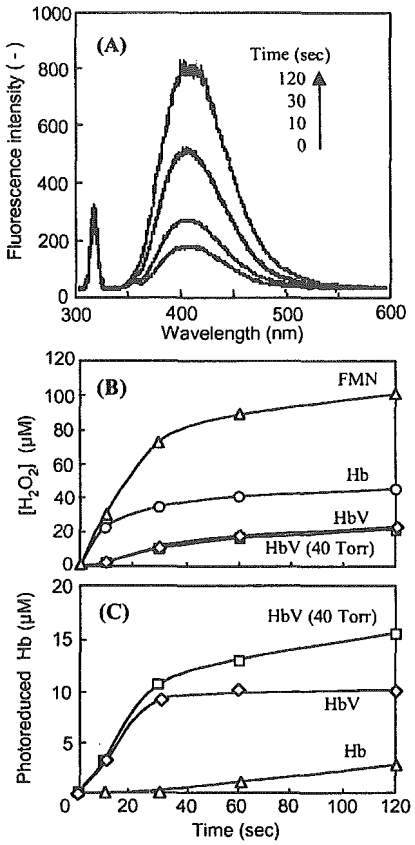

Figure 8. Detection of H_2O_2 using the fluorescence of DBDA during the photoreduction of Hb and HbV in the presence of FMN and EDTA. (A) An example of the fluorescence spectroscopy of the DBDA. The fluorescence intensity (λ_{em} = 404 nm) increased with time during the photoreduction of metHb solution under aerobic conditions (pO_2= 150 Torr). (B) Time course of the generation of H_2O_2 during the photoreduction of Hb and HbV under aerobic conditions (pO_2= 150 Torr), and HbV at pO_2 = 40 Torr. Irradiation to FMN alone was also tested as a reference (top curve) that produced 100 μM H_2O_2 for 120 s. Liberation of H_2O_2 from HbV was significantly suppressed in comparison with Hb solution. (C) The levels of metHb photoreduction during the measurement of H_2O_2 generation. The concentrations of heme (20 μM), FMN (5 μM), and EDTA (50 μM) in the cuvette were identical between the metHb solution and HbV suspension. For HbV, $[heme]_{in}$ = 21.6 mM, $[FMN]in$ = 5 mM, and $[EDTA]_{in}$ = 50 mM.

two propionic acid groups of a heme that directly face the outer aqueous phase of an Hb molecule should contribute to the electron transfer from the externally added FMN to the heme.

The side reaction of $FMNH_2$ is the reaction with O_2 to generate singlet O_2 ($^1O_2$) or H_2O_2 (*11*, *42*), due to the low redox potential of reduced flavin (E_m = −209 mV). However, according to the quantitative measurement of H_2O_2, photoreduction of metHbV significantly reduced the side reaction in comparison with the metHb solution. This effect is due to the highly concentrated condition inside metHbV: the photoexcited FMN* readily reacts with EDTA to generate $FMNH_2$, and it also readily reacts with concentrated metHb inside the HbV nanoparticle. However, for the complete removal of H_2O_2, further coencapsulation of catalase would be effective (*29*) in the presence of O_2. Of course, in the absence of O_2, only the metHb reduction proceeds.

We tried to find other optimal electron donors instead of EDTA, because it has been reported that the oxidized and decomposed EDTA elements contain acetaldehyde that might react with the lysine residues on a protein molecule (*10*), and EDTA is a strong chelator of Ca^{2+} as an anticoagulant and may require caution when using a large dosage. We confirmed that Met was effective secondary to EDTA, as reported by other researchers (*9*, *32*). Arg was also effective, but it was not stable against oxidation during incubation under aerobic conditions at 37 °C for 3 days. Met was stable against oxidation. However, the small amino acid, Met (Mw = 149), gradually leaks out from the HbV across the phospholipid bilayer membrane (data not shown). To minimize the leakage of an electron donor, larger molecules, Met-Met and Met-Glu, were tested. Unexpectedly, they did not show any contribution as an electron donor and retarded the reduction of FMN. The ribityl phosphate group in the FMN molecule can be an electron donor, because the photoreduction of FMN proceeds without the addition of an electron donor. The retardation by the peptides should be probably due to some interaction of these peptides with the ribityl phosphate group that may hinder the electron transfer to the isoalloxazine ring. Other amino acids such as Phe and Lys, and saccharides such as mannitol or maltotoriose, are effective as an electron donor; however, their reduction rates of FMN were much lower in comparison with EDTA. Interestingly, methanol and gaseous H_2 also showed facilitation. DTPA, a structure similar to EDTA, showed an effectiveness comparable with EDTA. EDTA is a well-known electron donor, and its larger size (Mw = 292) and four negative charges prevent leakage from the vesicles. We could not find a more effective electron donor in our study, but confirmed that IEF and native-PAGE did not demonstrate any change in the chemical modification of the photoreduced Hb in the presence of EDTA/FMN, and the O_2 binding property was successfully restored. Therefore, we tested coencapsulation of FMN/EDTA in HbV for the other studies.

When HbV is intravenously infused for the substitution of blood, the concentrations of Hb and the heme of HbV in plasma should reach 5 g/dL and 3.1 mM, respectively, or higher (*43*). These are much higher than the experimental conditions in Figures 1−4, and it is impossible to test such a highly concentrated solution in a cuvette because of the strong light scattering by the particles and absorption by Hbs. We thus tested sandwiching the solution with two glass plates, thus making a thin liquid layer between the glass plates. The thickness of the liquid membrane is approximately 10 μm, about twice the capillary diameter in in vivo peripheral tissues. Irradiation of visible light onto the liquid membrane of HbV coencapsulating FMN and EDTA showed significantly fast rates for the metHb photoreduction. Especially, the coencapsulation of FMN (5 mM) and EDTA (50 mM) completed the metHb photoreduction within only 20 s. This significantly fast photoreduction system would be applicable to the transcutaneous irradiation of visible light to the body for the rejuvenation of HbV when the metHb content increased after the infusion of HbV.

In our study we established an efficient photoreduction system in a nanoparticle as shown in Figure 9. The illuminated visible light excites FMN to convert it to FMN*, and this reacts with an electron donor and transforms to $FMNH_2$, that subsequently reduces ferric metHb to its ferrous form. The reduced Hb can then reversibly bind O_2. Irrespective of the blood substitutes, one advantage of coencapsulation in a nanoparticle is that the concentrations of the components in the vesicles (nanoenvironment) are very high. Accordingly, the desired reactions are significantly accelerated and the

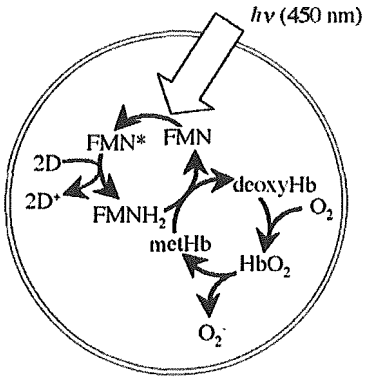

Figure 9. MetHb photoreduction system in a nanoparticle (HbV) using FMN and an electron donor (D), and recovery of the O_2-binding property.

unwanted side reaction is minimized in comparison with the homogeneous solution. To completely eliminate the side reaction of $FMNH_2$ and O_2, photoreduction under anaerobic conditions or coencapsulation of a radical scavenger, such as catalase, would be effective (*29*, *30*). RBC contains NADPH-flavin reductase to reduce metHb (*21*), and the reduced form of flavin is susceptible to react with O_2 as a side reaction. However, our results imply that the highly concentrated condition in RBCs and well-organized radical scavenging system should contribute to the effective metHb reduction in RBCs.

ACKNOWLEDGMENT

Supported by Health Sciences Research Grants (Research on Pharmaceutical and Medical Safety, Artificial Blood Project), the Ministry of Health and Welfare, Japan, 21 COE "Practical Nano-Chemistry" from MEXT, Japan, and Grants in Aid for Scientific Research from the Japan Society for the Promotion of Science (B16300162).

LITERATURE CITED

(1) Tracewell, C. A., Cua, A., Stewart, D. H., Bocian, D. F., and Brudvig, G. W. (2001) Characterization of carotenoid and chlorophyll photooxidation in photosystem II. *Biochemistry 40*, 193−203.

(2) Vorkink, W. P., and Cusanovivh, M. A. (1974) Photoreduction of horse heart cytochrome *c*. *Photochem. Photobiol. 19*, 205−215.

(3) Adar, F., and Yonetani, T. (1978) Resonance Raman spectra of cytochrome oxidase. Evidence for photoreduction by laser photons in resonance with the Soret band. *Biochim. Biophys. Acta 502*, 80−86.

(4) Kitagawa, T., and Nagai, K. (1979) Quaternary structure-induced photoreduction of haem of haemoglobin. *Nature 281*, 503−504.

(5) Kitagawa, T., Chihara, S., Fushitani, K., and Morimoto, H. (1984) Resonance Raman study of subunit assembly dependent photoreduction of heme of extracellular giant hemoglobin. *J. Am. Chem. Soc. 106*, 1860−1862.

(6) Pierre, J., Bazin, M., Debey, P., and Santus, P. (1982) One-electron photoreduction of bacterial cytochrome P-450 by ultraviolet light. *Eur. J. Biochem. 124*, 533−537.

(7) Sakai, H., Onuma, H., Umeyama, M., Takeoka, S., and Tsuchida E. (2000) Photoreduction of methemoglobin by irradiation in the near-ultraviolet region. *Biochemistry 39*, 14595−14602.

(8) McCormick, D. B., Koster, J. F., and Veeger, C. (1967) On the mechanism of photochemical reductions of FAD and FAD-dependent flavoproteins. *Eur. J. Biochem. 2*, 387−391.

(9) Heelis, P. F., Parsons, B. J., Phillips, G. O., and McKellar, J. F. (1979) The photoreduction of flavins by amino acids and EDTA. A continuous and flash photolysis study. *Photochem. Photobiol. 30*, 343−347.

(10) Traber, R., Kramer, H. E. A., and Hemmerich, P. (1982) Mechanism of light-induced reduction of biological redox centers by amino acids. A flash photolysis study of flavin photoreduction by ethylenediaminetetraacetate and nitrilotriacetate. *Biochemistry 21*, 1687−1693.

(11) Massey, V., Strickland, S., Mayhew, S. G., Howell, L. G., Engel, P. C., Matthews, R. G., Schuman, M., and Sullivan, P. A. (1969) The production of superoxide anion radicals in the reaction of reduced flavins and flavoproteins with molecular oxygen. *Biochem. Biophys. Res. Commun.* 36, 891−897.

(12) Massey, V., Stankovich, M., and Hemmerich, P. (1978) Light-mediaated reduction of flavoproteins with flavins as catalyst. *Biochemistry 17*, 1−8.

(13) Cusanovich, M. A., Meyer, T. E., and Tollin, G. (1985) Flavocytochrome *c*: Transient kinetics of photoreduction by flavin analogues. *Biochemistry 24*, 1281−1287.

(14) Sharp, R. E., Moser, C. C., Rabanal, F., and Dutton, P. L. (1998) Design, synthesis, and characterization of a photoactivatable flavocytochrome molecular maquette. *Proc. Natl. Acad. Sci. U.S.A.* 95, 10465−10470.

(15) Hazzard, J. T., Govindaraj, S., Poulos, T. L., and Tollin, G. (1997) Electron transfer between the FMN and heme domains of cytochrome P450 μ_B-3. *J. Biol. Chem. 272*, 7922−7926.

(16) Shumyantseva, V. V., Bulko, T. V., Schmid, R. D., and Archakov, A. I. (2002) Photochemical properties of a riboflavins/cytochrome P450 2B4 comples. *Biosensors Bioelecronics 17*, 233−238.

(17) Shumyantseva, V. V., Bulko, T. V., Schmid, R. D., and Archakov, A. I. (2000) Flavocytochrome P450 2B4 photoreduction. *Biophysics 45*, 982−987 (Translated from *Biofizika*).

(18) Masuda, S., and Bauer, C. E. (2002) AppA is a blue light photoreceptor that antirepresses photosynthesis gene expression in Rhodobacter sphaeroides. *Cell 110*, 613−623.

(19) Tsubota, K., Laing, R. A., and Kenyon, K. R. (1987) Noninvasive measurements of pyridine nucleotide and flavoprotein in the lens. *Invest. Ophthalmol. Vis. Sci. 28*, 785−789.

(20) Brown, W. D., and Synder, H. E. (1969) Nonenzymatic reduction and oxidation of myoglobin and hemoglobin by nicotinamide adenine dinucleotides and flavins. *J. Biol. Chem. 244*, 6702−6706.

(21) Yubisui, T., Takeshita, M., and Yoneyama, Y. (1980a) Reduction of methemoglobin through flavin at the physiological concetration by NADPH-flavin reductase of human erythrocytes. *J. Biochem. 87*, 1715−1720.

(22) Yubisui, T., Matsukawa, S., and Yoneyama, Y. (1980b) Stopped flow studies on the nonenzymatic reduction of methemoglobin by reduced flavin mononucleotide. *J. Biol. Chem. 255*, 11694−11697.

(23) Tsuchida, E. (1998) *Blood Substitutes: present and future perspectives* (Tsuchida, E., Ed.) Elsevier Science, New York.

(24) Takeoka, S., Ohgushi, T., Ohmori, T., Terase, T., and Tsuchida, E. (1996) Layer controlled hemoglobin vesicles by interaction of hemoglobin with phospholipid assembly. *Langmuir 12*, 1775−1779.

(25) Sakai, H., Takeoka, S., Park, S. I., Kose, T., Nishide, H., Izumi, Y., Yoshizu, A., Kobayashi, K., and Tsuchida, E. (1997) Surface modification of hemoglobin vesicles with poly(ethyleneglycol) and effects on aggregation, viscosity, and blood flow during 90% exchange transfusion in anesthetized rats. *Bioconjugate Chem. 8*, 23−30.

(26) Szebeni, J., Hauser, H., Eskelson, C. D., Watson, R. R., and Winterhalter, K. H. (1988) Interaction of hemoglobin derivatives with liposomes. Membrane cholesterol protects against the changes of hemoglobin. *Biochemistry 27*, 6425−6434,

(27) Takeoka, S., Sakai, H., Kose, T., Mano, Y., Seino, Y., Nishide, H., and Tsuchida, E. (1997) Methemoglobin formation in hemoglobin vesicles and reduction by encapsulated thiols. *Bioconjugate Chem. 8*, 539−544.

(28) Sakai, H., Tomiyama, K., Sou, K., Takeoka, S., and Tsuchida, E. (2000) Poly(ethyleneglycol)-conjugation and

deoxygenation enable long-term preservation of hemoglobin vesicles as oxygen carriers. *Bioconjugate Chem. 11*, 425−432

(29) Teramura, Y., Kanazawa, H., Sakai, H., Takeoka, S., and Tsuchida, E. (2003) The prolonged oxygen -carrying ability of Hb vesicles by coencapsulation of catalase in vivo. *Bioconjugate Chem. 14*, 1171−1176.

(30) D'Agnillo, F., and Chang, T. M. (1998) Polyhemoglobin-superoxide dismutase-catalase as a blood substitute with antioxidant properties. *Nat. Biotechnol. 16*, 667−71.

(31) Chang, T. M., Powanda, D., and Yu WP. (2003) Analysis of polyethylene-glycol-polylactide nano-dimension artificial red blood cells in maintaining systemic hemoglobin levels and prevention of methemoglobin formation. *Artif. Cells Blood Substitutes Immobilization Biotechnol. 31*, 231−47.

(32) Everse, J. (1994) Photochemical reduction of methemoglobin and methemoglobin derivatives. *Methods Enzymol. 231*, 524−536.

(33) Sakai, H., Takeoka, S., Yokohama, H., Seino, Y., Nishide, H., and Tsuchida, E. (1993) Purufication of concentrated Hb using organic solvent and heat treatment. *Protein Expression Purif. 4*, 563−569.

(34) Sakai, H., Yuasa, M., Onuma, H., Takeoka, S., and Tsuchida, E. (2000) Synthesis and physicochemical characterization of a series of hemoglobin-based oxygen carriers: objective comparison between cellular and acellular types. *Bioconjugate Chem. 11*, 56−64.

(35) Hatchard, C. G., and Parker, C. A. (1956) A new sensitive chemical actinometer II. Potasium ferrioxalate as a standard chemical actinometer. *Proc. R. Soc. London 235*, 518−536.

(36) Wegner, E. E., and Adamson, A. W. (1966) Photochemistry of complex ions. III. Absolute quantum yields for the photolysis of some aqueous chromium (III) complexes. Chemical actinometry in the long wavelength visible region. *J. Am. Chem. Soc. 88*, 394−404.

(37) Sou, K., Naito, Y., Endo, T., Takeoka, S., and Tsuchida, E. (2003) Effective encapsulation of proteins into size-controlled phospholipid vesicles using freeze−thawing and extrusion. *Biotechnol. Prog. 19*, 1547−1552.

(38) Sou, K., Endo, T., Takeoka, S., and Tsuchida, E. (2000) Poly(ethylene glycol)-modification of the phospholipid vesicles by using the spontaneous incorporation of poly(ethylene glycol)-lipid into the vesicles. *Bioconjugage Chem. 11*, 372−379.

(39) Sakai, H., Tomiyama, K., Masada, Y., Takeoka, S., Horinouchi, H., Kobayashi, K., and Tsuchida, E. (2003) Pretreatment of serum containing Hb-vesicels (oxygen carriers) to avoid interference in clinical laboratory tests. *Clin. Chem. Lab. Med. 41*, 222−231.

(40) Hamachi, I., Nomoto, K., Tanaka, S., Tajiri, Y., and Shinkai, S. (1994) Self-sufficient electron injection from NADH to the active center of flavin-pendant myoglobin. *Chem. Lett. 1994*, 1139−1142.

(41) Matsuo, T., Hayashi, T., and Hisaeda, Y. (2002) Reductive activation of dioxygen by a myoglobin reconstituted with a flavohemin.*J. Am. Chem. Soc. 124*, 11234−11235.

(42) Frati, E., Khatib, A., Front, P., Panasyuk, A., Aprile, F., and Mitrovic, D. R. (1997) Degradation of hyaluronic acid by photosensitized riboflavin in vitro. Modulation of the effect by transition metals, radical quenchers, and metal chelators. *Free Rad. Biol. Med. 22*, 1139−1144.

(43) Sakai, H., Horinouchi, H., Masada, Y., Yamamoto, M., Takeoka, S., Kobayashi, K., Tsuchida, E. (2004) Hemoglobin-vesicles suspended in recombinant human serum albumin for resuscitation from hemorrhagic shock in anesthetized rats. *Crit. Care Med. 32*, 539−545.

BC049913Z

0022-3565/04/3113-874–884$20.00
THE JOURNAL OF PHARMACOLOGY AND EXPERIMENTAL THERAPEUTICS
Copyright © 2004 by The American Society for Pharmacology and Experimental Therapeutics
JPET 311:874–884, 2004

Vol. 311, No. 3
73049/1179358
Printed in U.S.A.

Physiological Capacity of the Reticuloendothelial System for the Degradation of Hemoglobin Vesicles (Artificial Oxygen Carriers) after Massive Intravenous Doses by Daily Repeated Infusions for 14 Days

Hiromi Sakai, Yohei Masada, Hirohisa Horinouchi, Eiji Ikeda, Keitaro Sou, Shinji Takeoka, Makoto Suematsu, Masuhiko Takaori, Koichi Kobayashi, and Eishun Tsuchida

Advanced Research Institute for Science and Engineering (H.S., Y.M., K.S., S.T., E.T.), Waseda University, Tokyo, Japan; Departments of Surgery (H.H., K.K.), Pathology (E.I.), and Biochemistry (M.S.), School of Medicine, Keio University, Tokyo, Japan; and East Takarazuka Satoh Hospital (M.T.), Takarazuka, Japan

Received June 21, 2004; accepted August 4, 2004

ABSTRACT

A hemoglobin vesicle (HbV; diameter 252 ± 53 nm) or liposome-encapsulated Hb is an artificial oxygen carrier developed for use as a transfusion alternative, and its oxygen-transporting capacity has been well characterized, although critical physiological compartments for the Hb degradation after a massive infusion of HbV and the safety outcome remain unknown. In this study, we aimed to examine the compartments for its degradation by daily repeated infusions (DRI) of HbV, focusing on its influence on the reticuloendothelial system (RES). Male Wistar rats intravenously received the HbV suspension at 10 ml/kg/day for 14 consecutive days. The cumulative infusion volume (140 ml/kg) was equal to 2.5 times the whole blood volume (56 ml/kg). The animals tolerated the DRI well and survived, and body weights continuously increased. One day after DRI, hepatosplenomegaly occurred significantly through the accumulation of large amounts of HbV. Plasma clinical chemistry was overall normal, except for a transient elevation of lipid components derived from HbV. These symptoms subsided 14 days after DRI. Hemosiderin deposition and up-regulation of heme oxygenase-1 coincided in the liver and spleen but were not evident in the parenchyma of these organs. Furthermore, the plasma iron and bilirubin levels remained unchanged, suggesting that the heme-degrading capacity of the RES did not surpass the ability to eliminate bilirubin. In conclusion, phospholipid vesicles for the encapsulation of Hb would be beneficial for heme detoxification through their preferential delivery to the RES, a physiological compartment for degradation of senescent RBCs, even at doses greater than putative clinical doses.

Phospholipid vesicles or liposomes have been extensively studied as a carrier of functional (macro)molecules for a drug delivery system, and some are now approved for clinical use as antifungal or anticancer therapies (Lian and Ho, 2001). Vesicles encapsulating concentrated hemoglobin (Hb), so-called Hb vesicles (HbV) or liposome-encapsulated Hb, have been developed as artificial oxygen carriers, and their sufficient ability to transport oxygen comparable with blood has been well clarified (Djordjevich et al., 1987; Chang et al., 1992; Izumi et al., 1997; Phillips et al., 1999; Sakai et al., 2004c). The advantages of an artificial oxygen carrier are the absence of blood-type antigens and transfusion-related transmission of infections, and stability during long-term storage. In this sense, the infusion of oxygen carriers becomes superior to the conventional blood transfusion that still has the potential of mismatching, the risk of infections secondary to the infusion of contaminated blood, and the problem of only a few weeks' storage life.

In a series of safety studies of HbV, it has been clarified that the cellular structure and the size of the HbV are advantageous for maintaining a steady blood circulation with-

This work was supported by Health Sciences Research grants (Research on Pharmaceutical and Medical Safety, Artificial Blood Project); the Ministry of Health, Labor and Welfare, Japan; grants-in-aid for Scientific Research from the Japan Society for the Promotion of Science (B16300162); 21 COE "Practical Nano-Chemistry" from the Ministry of Education, Culture, Sports, Science and Technology of Japan; and Oxygenix Inc. (Tokyo, Japan). S.T., M.S., K.K., and E.T. are consultants of Oxygenix Inc.

Article, publication date, and citation information can be found at http://jpet.aspetjournals.org.

doi:10.1124/jpet.104.073049.

ABBREVIATIONS: HbV, Hb vesicle(s); Hct, hematocrit; RES, reticuloendothelial system; PEG, poly(ethylene glycol); RBC, red blood cell; DRI, daily repeated infusion(s); DPPC, 1,2-dipalmitoyl-*sn*-glycero-3-phosphatidylcholine; DHSG, 1,5-*O*-dihexadexyl-*N*-syccynyl-L-glutamate; MAP, mean arterial pressure; HR, heart rate; UA, uric acid; BUN, urea nitrogen; CRE, creatinine; PT, prothrombin time; APTT, activated partial thromboplastin time; HO-1, heme oxygenase-1.

out vasoconstriction and hypertension (Sakai et al., 2000a) and that the surface modification of HbV with polyethylene glycol (PEG) is beneficial not only for a longer circulation time (Phillips et al., 1999) but also for suppression of intervesicular aggregation of HbV during preservation for years and in the plasma phase in the peripheral tissues after intravenous infusion (Sakai et al., 1998, 2000b). In our previous report on the histopathological analysis of rats receiving a bolus HbV infusion (20 ml/kg), the HbV particles are recognized as foreign materials and finally captured mainly by the reticuloendothelial system (RES, or mononuclear phagocytic system) in the spleen and liver, and they are promptly degraded (Sakai et al., 2001). These are outstanding characteristics in comparison with molecular Hb that shows a shorter circulation time because it is filtered through the kidneys when the Hb concentration exceeds the haptoglobin concentration and induces hemoglobinuria and eventually renal failure, and it extravasates across the fenestrated endothelium in the liver and induces excess heme catabolism in the hepatocytes and marked sinusoidal constriction (Goda et al., 1998, Kyokane et al., 2001). However, it is not clear whether the physiological capacity of the RES for the degradation and excretion of the components of HbV would be sufficient even after a massive infusion of HbV. The circulation half-life of HbV is within a few days, which is significantly shorter than that of red blood cells (RBCs), and it is anticipated that a massive infusion of HbV would burden the RES and result in abrupt heme degradation and iron overload having the potential to cause deleterious effects.

One of the safety studies of a new drug in the preclinical stage should be a massive dose by daily repeated infusions (DRI) in rodents and nonrodents for at least 14 days at three different dosages; a guideline decided by the International Conference on Harmonization of Technical Requirements for Registration of Pharmaceuticals for Human Use. However, the documentation of the DRI studies to the public is scarce, especially in the research field of artificial oxygen carriers (Biro and Greenburg, 1999). In a clinical setting, the amount of an artificial oxygen carrier to be infused should be at least several hundred milliliters, which is significantly greater than the dose of conventional drugs; therefore, it is not clear whether a preclinical protocol for a conventional drug is appropriate for the safety evaluation of artificial oxygen carriers. On the other hand, there may be a need for a repetitive infusion of an oxygen carrier in a clinical situation, such as chronic anemia (Hamilton et al., 2001) or cancer therapy (Teicher et al., 1997). Based on these backgrounds, we tested the DRI of HbV into Wistar rats at one dose rate as a preliminary study to confirm the safety of HbV. Because the dose amount of phospholipid vesicles for use as an oxygen carrier is significantly greater than that used for conventional drugs, the influence of a massive infusion of HbV on the RES and the excretion of the components, especially after heme degradation, are of great concern.

Materials and Methods

Preparation of HbV Suspension. The test fluid, the HbV suspension, was prepared under sterile conditions as reported previously (Sakai et al., 2000b; Sou et al., 2000, 2003). Human Hb was purified from outdated, donated blood provided by the Hokkaido Red Cross Blood Center (Sapporo, Japan) and the Japanese Red Cross Society (Tokyo, Japan). The encapsulated Hb (38 g/dl) contained 14.7 mM pyridoxal 5′-phosphate (Aldrich Chemical Co., Milwaukee, WI) as an allosteric effector at a molar ratio of pyridoxal 5′-phosphate/Hb = 2.5. The lipid bilayer was composed of a mixture of 1,2-dipalmitoyl-*sn*-glycero-3-phosphatidylcholine (DPPC), cholesterol, and 1,5-*O*-dihexadecyl-*N*-succynyl-L-glutamate (DHSG) at a molar ratio of 5:5:1 (Nippon Fine Chemicals Co., Osaka, Japan), and 1,2-distearoyl-*sn*-glycero-3-phosphatidylethanolamine-*N*-PEG_{5000} (NOF Co., Tokyo, Japan). Thus, the vesicular surface is covered with PEG chains. The molar composition of DPPC/cholesterol/DHSG/1,2-distearoyl-*sn*-glycero-3-phosphatidylethanolamine-*N*-PEG_{5000} was 5:5:1:0.033. HbVs were suspended in a physiological salt solution, sterilized using filters (pore size, 0.45 μm, Dismic; Toyo Roshi Co., Tokyo, Japan), and deoxygenated with bubbling N_2 for storage (Sakai et al., 2000b). The physicochemical parameters of the HbV are as follows: particle diameter, 252 ± 53 nm; [Hb], 9.5 g/dl; [metHb], 2.3%; [HbCO], <2%; [lipids], 5.3 g/dl; and oxygen affinity (P_{50}), 30 Torr. The endotoxin content was measured by a modified *Limulus* amebocyte lysate gel-clotting analysis (Wako Pure Chemicals, Tokyo, Japan) and was less than 0.2 endotoxin unit/ml (Sakai et al., 2004a).

In our previous reports on resuscitation from hemorrhagic shock or extreme hemodilution, the HbV was suspended in a 5-g/dl albumin solution as a plasma expander to regulate the colloid osmotic pressure to 20 mm Hg (Sakai et al., 2004c). However, it is anticipated that the DRI of HbV suspended in albumin would result in enhanced hypervolemia. Because the main purpose of this DRI study was to clarify the safety of HbV and not albumin, HbV was simply suspended in a physiological saline solution.

Daily Repeated Infusion of HbV. All animal studies were approved by the Animal Subject Committee of the Keio University School of Medicine and performed according to National Institutes of Health Guidelines for the Care and Use of Laboratory Animals (NIH Publication #85-23 rev. 1985).

The experiments were carried out using 34 male Wistar rats (145 ± 4 g; Saitama Experimental Animals, Kawagoe, Japan). All the rats were housed in cages and provided with food and water ad libitum in a temperature-controlled room on a 12-h dark/light cycle. At first, the rats were anesthetized lightly with diethyl ether inhalation and then 1.5% sevoflurene (Maruishi Pharmaceutical Co., Osaka, Japan) using a vaporizer (model TK-4 Biomachinery; Kimura Medical, Tokyo, Japan) to immobilize them for every infusion. Every day for 14 days, the rats received HbV (n = 12) or saline (n = 12) via the tail vein using an indwelling needle (24-gauge; Nipro Co., Osaka, Japan) at a dose rate of 10 ml/kg with an injection rate of 1 ml/min. The total volume of the infused HbV into a rat for 14 days reached 140 ml/kg, which was equal to 2.5 times the actual blood volume of the rat (56 ml/kg). The infused total solid material (Hb and lipids) is calculated to be 20,689 mg/kg (1478 mg/kg/day × 14 days). The rats were weighed every day just before every infusion to calculate the amount of the infusion. After every infusion, the needle was immediately removed and the bleeding was stopped by applying pressure for a short time. The two groups (n = 12) were divided in half (n = 6 × 2), and six rats were sacrificed 1 day after the final 14th infusion. The remaining six rats were sacrificed at 14 days after the final infusion. Ten animals without the infusions were used to obtain control values.

Hematological Test. A hematological examination was performed at 1, 3, 7, 9, and 12 days during the DRI and at 1, 7, and 14 days after the final infusion. About 200 μl of blood was collected from a tail vein when an indwelling needle was inserted for HbV infusion. Seventy microliters was immediately diluted with 200 μl of citrate solution for a blood cell counter (Sysmex KX-21, Kobe, Japan), and the rest of the blood was inserted into a glass capillary (Terumo Co., Tokyo, Japan) for hematocrit (Hct) measurements. In this study, Hct indicates the volume of RBC and does not include the volume of HbV. The concentration of HbV in the plasma was measured by a cyanomethemoglobin method.

Hemodynamic and Blood Gas Parameters, Blood Glucose Level, and Urinalysis. One day or 2 weeks after the final infusion, the rats were anesthetized with 1.5% sevoflurene inhalation. A polyethylene tube (PE-50; Natsume Co., Tokyo, Japan) was inserted into the carotid artery for measurement of the mean arterial pressure (MAP), the heart rate (HR) by a recording system (Polygraph system 1000; Nippon Koden, Tokyo, Japan) and for withdrawing blood for various measurements. For the blood gas analysis, blood samples were collected in 70 IU/ml heparinized microtubes (125 μl, Clinitubes; Radiometer Nederland, Copenhagen, Denmark) and injected into a pH/blood gas analyzer (model ABL 555; Radiometer Nederland) for analyses of the arterial blood O_2 tension, arterial blood carbon dioxide tension, pH, base excess, and lactate. The blood glucose level was measured with a Medisafe Reader (GR-101; Terumo Co., Tokyo, Japan). Urinalysis was performed by dip-stick-testing (UA-L08M; Terumo Co.) as a qualitative measurement. A urine specimen of a rat was collected in a transparent plastic bag when the rat was lightly anesthetized with diethyl ether, and a test stick was dipped in the collected urine. In each item, the levels were judged by visual examination of the color identification after a specific time of exposure according to the instructions, in the order of protein (10 s), pH (10 s), occult blood (20 s), ketone body (20 s), urobilinogen (20 s), glucose (30 s), nitrite (30 s), and bilirubin (40 s).

Plasma Clinical Chemistry. A part of the withdrawn blood (6 ml) was centrifuged to obtain plasma that was turbid and red/brown colored due to the presence of PEG-modified HbV particles, especially in the samples taken one day after DRI. The plasma was ultracentrifuged (50,000*g*; 20 min) to remove the HbV particles (Sakai et al., 2003). The obtained transparent plasma specimens were stored in a freezer at −80°C until the clinical chemistry tests (BML, Kawagoe, Japan). The selected analytes were total protein, albumin, total bilirubin, aspartate aminotransferase, alanine aminotransferase, γ-glutamyltransferase, alkaline phosphatase, cholinesterase, leucine amino peptidase, creatine phosphokinase, amylase, lipase, aldosterone, total cholesterol, cholesterol ester, free cholesterol, HDL-cholesterol, β-lipoprotein, triglyceride, free fatty acid, phospholipids, total lipids, uric acid (UA), urea nitrogen (BUN), creatinine (CRE), K^+, Ca^{2+}, inorganic phosphate, unsaturated iron binding capacity, and Fe^{3+}. All the analytical methods were described in our previous articles (Sakai et al., 2003, 2004b).

Blood Coagulation Test and Fibrinogen Concentration. For the blood coagulation test at 1 and 14 days after the final infusion of HbV or saline, 1.8 ml of the withdrawn blood was immediately mixed with 0.2 ml of 3.8% sodium citrate solution. The plasma fraction, obtained by gentle centrifugation, was analyzed for prothrombin time (PT), activated partial thromboplastin time (APTT), and fibrinogen (BML).

Histopathological Examination. The animals were finally laparotomized and sacrificed by acute bleeding from the abdominal aorta, and the liver, spleen, and kidney were resected for weight measurements and also all the other organs were obtained for a histopathological study. They were fixed in 10% buffered formalin (Wako Pure Chemicals) immediately after removal, and the paraffin sections were stained with hematoxylin & eosin, and Berlin blue.

Immunohistochemistry was performed to detect rat heme oxygenase-1 (HO-1) and human Hb from the injected HbV in the rat spleen and liver. Four-micrometer-thick paraffin sections were mounted on 3-aminopropyl triethoxysilane-coated glasses. The sections were treated with 0.03% H_2O_2 in methanol for 10 min at room temperature to block the endogenous peroxidase activity. For antigen retrieval, the sections were also treated with proteinase K (0.4 mg/ml; DakoCytomation California Inc., Carpinteria, CA) for 10 min at room temperature. After blocking the nonspecific binding with 5% normal goat serum, they were incubated with mouse monoclonal antibody against rat HO-1 (20 μg/ml; GTS-3, TaKaRa, Tokyo, Japan) at 4°C overnight. They were then incubated for 30 min at room temperature with goat antibodies against mouse immunoglobulins conjugated to the amino acid polymer [no dilution; Histofine Simple Stain MAX-PO(M), Nichirei Co., Tokyo, Japan]. Color was developed with 3,3′-diaminobenzidine tetrahydrochloride (0.2 mg/ml; Dojindo Laboratories, Kumamoto, Japan) in 0.05 M Tris-HCl, pH 7.4, containing 0.003% hydrogen peroxide. Subsequently, the sections were treated with 5% normal swine serum for 30 min at room temperature and reacted with rabbit polyclonal antibodies against human Hb (1:500 dilution; DakoCytomation A/S, Glostrup, Denmark) for 60 min at room temperature. They were further incubated with alkaline phosphatase-conjugated swine antibodies against rabbit immunoglobulins (1:100 dilution; DakoCytomation A/S). Color development was performed using a New Fuchsin Substrate kit (Nichirei Co.), and the sections were counterstained with hematoxylin.

Data Analysis. Differences between the control and the treatment group were analyzed using a one-way analysis of variance followed by Fisher's protected least significant difference test. The changes were considered statistically significant if $p < 0.05$. All the data are shown as mean ± S.D. For the results of the plasma clinical chemistry, the allowance of twice the standard deviation (2× S.D.) of the baseline values is indicated in the figures in considering the variable nature of these parameters.

Results

Body Weight. The body weight of rats in the HbV group (baseline, 144 ± 3 g) showed a monotonous increase during the 14 days of the DRI period and reached 195 ± 12 g (Fig. 1); however, this was slightly but significantly suppressed ($p < 0.05$) in comparison with the control saline group (220 ± 13 g). The body weight in the HbV group increased to 265 ± 14 g at 14 days after DRI. No significant difference was noted in the body weight compared with that of the saline control group (280 ± 22 g).

Hematological Changes and Concentration of HbV in Blood. The Hct of the HbV group (baseline, 41.7 ± 2.1%) tended to decrease to 37.5 ± 0.9% 1 day after DRI, which was lower than that of the saline group (44.7 ± 2.0%) (Fig. 2). However, after 14 days, the Hct of the HbV group increased to 45.1 ± 1.9%, which was comparable with that of the saline group (47.8 ± 2.7%). The numbers of white blood cells and platelets were comparable with those of the saline control group throughout the observation period.

The concentration of HbV immediately after every infusion was estimated from the volumes of the whole blood (56 ml/kg) and the infused volume of HbV (10 ml/kg) and was plotted

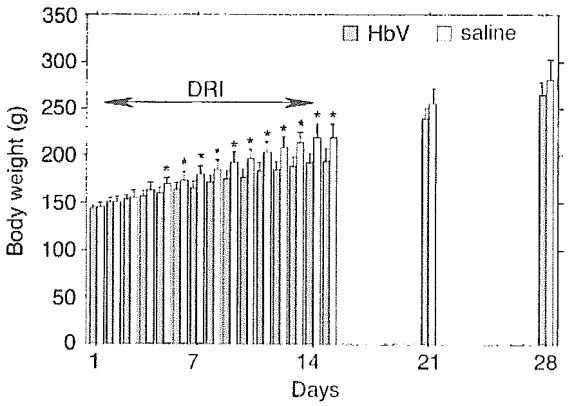

Fig. 1. Time course of the gain in body weight during and after DRI of HbV and saline for 14 days at a dose rate of 10 ml/kg/day. Both groups showed monotonous increases; however, after the 5th day, a significant difference was observed. Seven days after the final infusion, there were no significant differences between the two groups. The values are mean ± S.D. *, significantly different between the groups ($p < 0.05$).

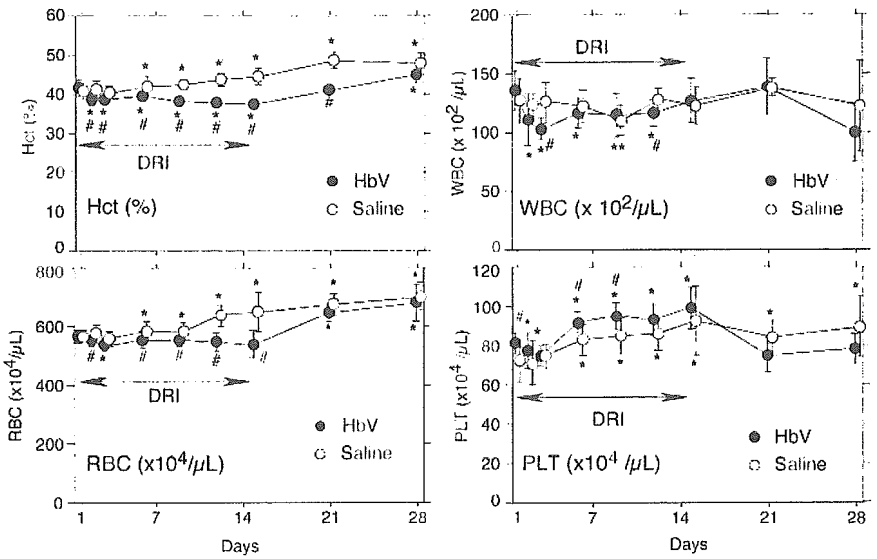

Fig. 2. Time course of Hct and blood cell counts during and after DRI of HbV and saline for 14 days at a dose rate of 10 ml/kg/day. The values are mean ± S.D. #, significantly different between the groups ($p < 0.05$). *, significantly different versus the baseline values ($p < 0.05$).

with open circles, and the measured concentration of HbV just before every infusion was plotted with solid circles (Fig. 3). The concentration of HbV just after the first infusion was estimated to be about 3 g/dl, and 1 day later, it decreased to 1.3 g/dl, with a half-life of about 22 h. The half-life of the second infusion seemed to become shorter. The DRI resulted in the accumulation of HbV in the plasma and it increased to 5.2 g/dl 1 day after the 14th infusion. However, 1 week after the final infusion, no HbV was confirmed in the plasma, indicating that all of the HbV was captured by the RES.

Coagulation Test. A coagulation test indicated that the HbV group showed a slight prolongation in APTT from 24.3 ± 1.3 s at the baseline to 36.0 ± 11.8 s 1 day after the DRI but changed to 40.3 ± 20.3 s after 14 days with marked individual variations. On the other hand, there was no noticeable change in the PT for the HbV group (Fig. 4). The fibrinogen concentration (baseline, 223 ± 12 mg/dl) significantly increased for all groups (HbV group, 1 day after DRI,

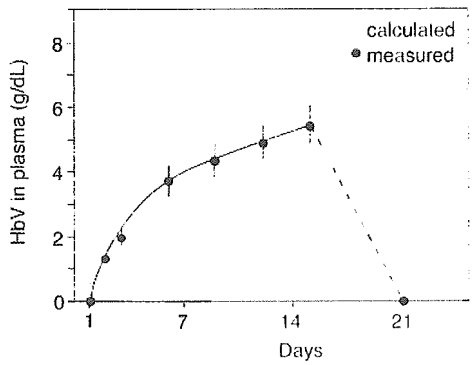

Fig. 3. Time course of the HbV concentration in the plasma phase during and after DRI of HbV for 14 days at a dose rate of 10 ml/kg/day. It is assumed that immediately after the first infusion, the concentration should be around 3 g/dl, and 1 day later, it decreased to about 1.2 g/dl. Immediately after the second infusion, the concentration should be about 4.3 g/dl and decreased to 2 g/dl 1 day later. The half-life of the HbV apparently decreases with multiple infusions. The concentration tended to reach a plateau. The final HbV concentration reached 5.3 g/dl, and this completely disappeared 7 days after DRI.

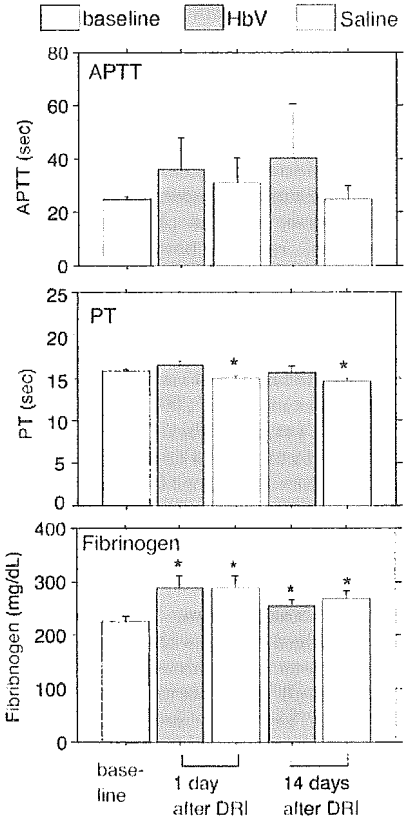

Fig. 4. Parameters for blood coagulation, APTT and PT, and fibrinogen concentration after DRI of HbV and saline for 14 days at a dose rate of 10 ml/kg/day. The values are mean ± S.D. *, significantly different versus the baseline group ($p < 0.05$).

289 ± 22 mg/dl; 14 days after DRI, 255 ± 11 mg/dl), probably due to the stress of infusion and influence on the liver function.

Blood Pressure, Heart Rate, and Blood Gas Parameters. Table 1 summarizes the blood gas parameters, blood glucose level, MAP, and HR 1 day after the DRI of HbV. There is no abnormal value except for an increase in MAP of

TABLE 1
Blood gas parameters, blood glucose level, MAP, and HR 1 and 14 days after DRI of HbV
Baseline values are also listed. The values are mean ± SD.

Parameters	1 Day after DRI	14 Days after DRI	Baseline
pH	7.44 ± 0.03	7.43 ± 0.03	7.48 ± 0.30
$PaCO_2$ (torr)	41 ± 3	44 ± 4	37 ± 4
PaO_2 (torr)	76 ± 4	75 ± 7	82 ± 7
Lactate (mM)	0.93 ± 0.12	0.88 ± 0.38	1.59 ± 0.45
Base excess (mM)	3.1 ± 1.3	4.0 ± 0.8	4.5 ± 1.3
Glucose (mg/dl)	147 ± 24	127 ± 9	146 ± 10
MAP (mm Hg)	125 ± 4*	111 ± 12	101 ± 8
HR (beats/min)	419 ± 10	402 ± 33	404 ± 42

* Significantly different versus the baseline group ($p < 0.05$).

the HbV group 1 day after DRI (125 ± 4 mm Hg) in comparison with the baseline value (101 ± 8 mm Hg).

Urinalysis. The color of the urine was normal for all groups, and there was no sign of hemoglobinurea. Table 2 summarizes the results of the urinalysis. The HbV group showed a slight increase in the protein concentration. There were no significant signs of any organ damage. Urobilinogen and bilirubin were within the normal range in spite of the large amount of HbV infusion.

Organ Weights. The liver and spleen are thought to be the main organs that trap and degrade HbV. As shown in Fig. 5, significant splenomegaly and hepatomegaly were confirmed 1 day after DRI. The percentage of spleen weight relative to the body weight increased from 0.33 ± 0.04% at the baseline to 0.94 ± 0.07 1 day after DRI, about 2.9 times the baseline value. This returned to 0.41 ± 0.03% after 14 days. The percentage of liver weight relative to the body weight increased from 4.81 ± 0.15% at the baseline to 5.83 ± 0.37% 1 day after DRI; and it returned to 4.33 ± 0.20%, comparable with the baseline after 14 days. The color of the liver was darkened just after DRI, however, it returned to its normal color 14 days after DRI. The kidney weight did not show any significant increase but tended to show a slight decrease for all groups.

Plasma Clinical Chemistry. A significant amount of the HbV particles was present in the plasma one day after DRI. However, they could be easily removed from the plasma by ultracentrifugation (50,000g; 20 min) (Sakai et al., 2003), and we could avoid any interference effect of HbV in the colorimetric and turbidimetric analyses in the plasma clinical chemistry. The parameters affecting the liver function (total

TABLE 2
The results of urinalysis for the HbV and saline control groups 1 and 14 days after DRI ($n = 6$)
The numbers indicate the counts of rats. Interpretation of judgment for the reading levels: protein (mg/dl), − (negative), ± (15), + (30), ++ (100), +++ (250), and ++++ (1000); occult blood (counts/μl), − (negative), + (10), ++ (50), and +++ (250); ketone body (mg/dl), − (negative), + (10), ++ (50), and +++ (100); urobilinogen (mg/dl), − (negative), ± (0.5), + (2), ++ (4), and +++ (8); glucose (mg/dl), − (negative), ± (50), + (150), ++ (500), and +++ (2000); nitrite, − (negative), and + (0.03–0.2 mg/dl); and bilirubin (mg/dl), − (negative), + (0.5), ++ (1), and +++ (2.5).

Parameters	Levels	1 Day after DRI		14 Days after DRI		Baseline
		HbV	Saline	HbV	Saline[a]	
Protein	−	0	1	2	0	2
	±	4	5	1	2	4
	+	2	0	2	2	0
	++	0	0	1	1	0
	+++	0	0	0	0	0
	++++	0	0	0	0	0
pH	5	0	2	0	0	0
	6	6	2	2	2	0
	7	0	1	4	2	5
	8	0	1	0	1	1
	9	0	0	0	0	0
Occult blood	−	3	2	4	3	4
	+	3	4	2	1	1
	++	0	0	0	1	1
	+++	0	0	0	0	0
Ketone body	−	0	0	0	0	0
	+	6	6	5	5	6
	++	0	0	1	0	0
	+++	0	0	0	0	0
Urobilinogen	−	0	0	0	0	0
	±	6	6	6	5	6
	+	0	0	0	0	0
	++	0	0	0	0	0
Glucose	−	6	6	6	5	6
	±	0	0	0	0	0
	+	0	0	0	0	0
	++	0	0	0	0	0
Nitrite	−	6	6	6	5	6
	+	0	0	0	0	0
Bilirubin	−	6	6	6	5	5
	±	0	0	0	0	1
	+	0	0	0	0	0
	++	0	0	0	0	0
	+++	0	0	0	0	0

[a] $n = 5$.

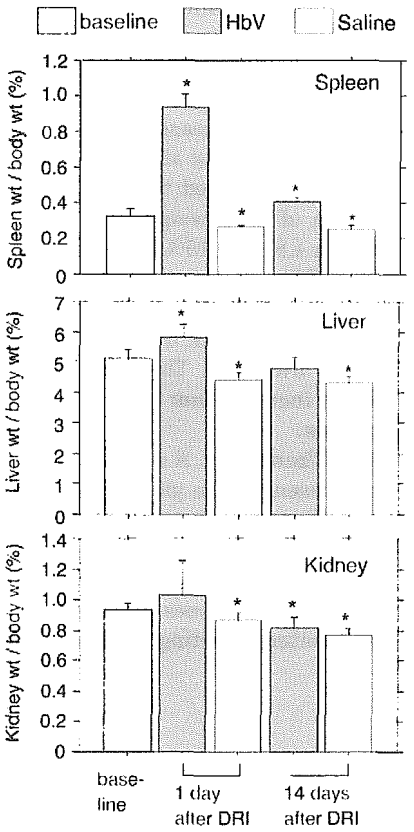

Fig. 5. Changes in organ weights (spleen, liver, and kidney) after DRI of HbV and saline for 14 days at a dose rate of 10 ml/kg/day. The values are mean ± S.D. *, significantly different versus the baseline group ($p < 0.05$).

protein, albumin, aspartate aminotransferase, alanine aminotransferase, leucine amino peptidase, alkaline phosphatase, γ-glutamyltransferase, and cholinesterase) did not show any noteworthy changes in the HbV group (Fig. 6).

The parameters affecting the function of the kidneys (CRE, uric acid, and BUN) varied within the normal ranges. The parameter reflecting the heart and skeletal muscle, creatine phosphokinase, did not show any noticeable change. Aldosterone, released from adrenal gland to regulate ionic balance, did not show noticeable change. A significant change was observed for the parameters of pancreatic function. In the HbV group, the lipase activity (baseline, 8.5 ± 1.4 U/l) increased to 48.5 ± 16.8 U/l 1 day after DRI and tended to decrease to 33.2 ± 29.4 U/l after 14 days. On the contrary, amylase activity (baseline, 1613 ± 74 U/l) did not show an increase but a slight decrease to 1455 ± 28 U/l 1 day after DRI and returned to 1546 ± 77 U/l after 14 days.

The concentrations of the cholesterol components (total and free cholesterols, and cholesterol ester) and lipids (β-lipoprotein, total lipids, and phospholipids) significantly increased 1 day after the final infusion (Fig. 7). For example, total cholesterol (baseline, 72.6 ± 7.5 mg/dl) increased to 182.2 ± 22.6 mg/dl after DRI. However, they returned to the original values 14 days after DRI. These increases should indicate that cholesterol and phospholipid (probably DPPC) are released from the RES after entrapping the HbV particles. Bilirubin and ferric iron, which should be released from the Hb decomposition, were minimal. Unsaturated iron binding capacity did not show noticeable changes. The electrolyte concentrations varied within the normal range.

Histopathological Examination. Histopathological examination 1 day after DRI showed a significant amount of HbV accumulated in the red pulp zone in the spleen, and very few RBCs were seen (Fig. 8a). In the liver, the presence of Kupffer cells that captured a large amount of HbV was seen (Fig. 8b). In the kidneys, the mesangial cells in the renal glomerulus seemed to entrap HbV (Fig. 8c). These organs and the adrenal gland were slightly stained with Berlin blue (data not shown), indicating that the decomposition of heme should have already started. No morphological change was noted in the myocardium; however, some slightly stained particles were observed (Fig. 8d). The pancreas (Fig. 8e), lungs (Fig. 8f), intestine, stomach, brain, thymus, testis, and skin did not show significant abnormalities.

Fourteen days after DRI, the images of the accumulated HbV almost disappeared in all organs. However, there were materials that were moderately stained with Berlin blue in the red pulp zone of the spleen (Fig. 9a), liver (Fig. 9b), bone marrow (Fig. 9c), and slightly in the kidney (Fig. 9d) and adrenal gland (Fig. 9e)

Immunohistochemical analysis of the liver and the spleen clarified the presence of human Hb in HbV as pink-colored areas that were stained with anti-human Hb-antibody 1 day after DRI (Fig. 10, a and b). In the spleen, the presence of HO-1 was confirmed as brown-colored stains in the cytoplasm of the macrophages in the red pulp zone both at 1 and 14 days after DRI (Fig. 10, a and c). In the liver, the presence of HO-1 was confirmed in the Kupffer cells only at 14 days after DRI (Fig. 10d). No HO-1 was confirmed in the parenchyma of these organs.

Discussion

Our primary finding is that all the rats tolerated the DRI of HbV well for 14 days with no deteriorative signs in organ functions, due to the preferable effect of Hb encapsulation in phospholipid vesicles that minimizes the toxicity of molecular Hbs and delivers them to the RES as a physiological compartment for degradation and detoxification of foreign materials. The RES had sufficient capacity for the degradation of HbV, even though the total infused volume reached 140 ml/kg, which was equal to 2.5 times the actual blood volume of the rat (56 ml/kg) and was significantly larger than the dose of multiple infusions of liposomes for antifungal and antitumor targeting (Fielding et al., 1999; Charrois and Allen, 2003).

The body weight of the HbV group monotonously increased, whereas the rate was slightly slower than that of the saline control group. It is speculated that the infusion of HbV, which could not be excreted easily in the urine and remain in circulation, could 1) disturb physiological functions and suppress the growth of the animals, 2) put the animals under stress and reduce their appetite, or 3) tend to accelerate the catabolism. In spite of such a condition, the components of HbV could be used as a part of the cellular components for the growth of rats. One and 2 weeks after DRI, there was no significant difference in the body weight between the groups.

The numbers of RBCs, whole blood cells, and platelets showed moderate changes, even though there were some

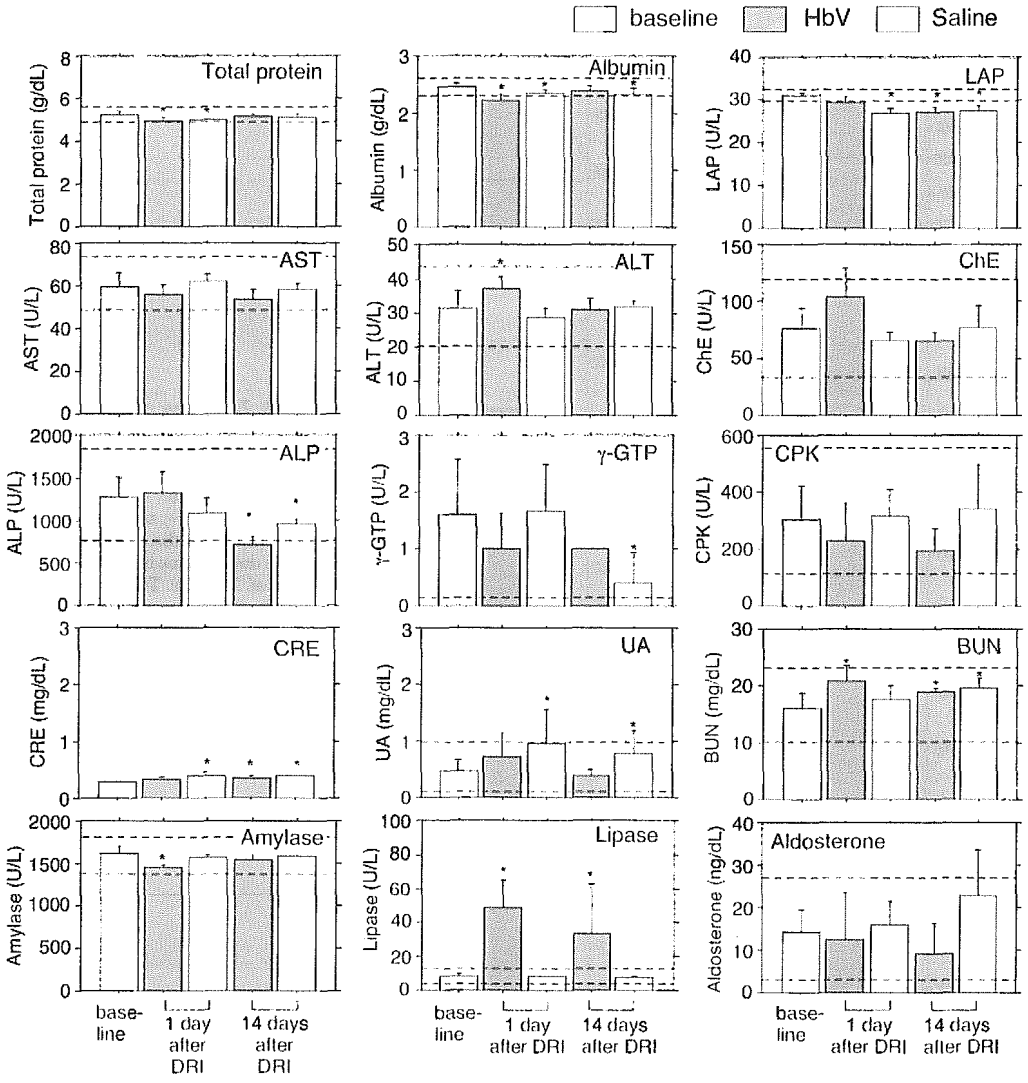

Fig. 6. Plasma clinical chemistry tests reflecting the organ functions such as liver, pancreas, and kidneys and the metabolism of Hb after DRI of HbV or saline. The values are mean ± S.D. *, significantly different versus the baseline group ($p < 0.05$). The dotted lines indicate the levels of 2× S.D. LAP, leucin amino peptidase; AST, aspartate aminotransferase; ALT, alanine aminotransferase; ChE, cholinesterase; ALP, alkaline phosphatase; γ-GTP, γ-glutamyltransferase; CPK, creatine phosphokinase; CRE, creatinine; UA, uric acid; BUN, urea nitrogen.

significant differences between the HbV and the saline groups. Hct and RBC counts decreased significantly for the HbV group, probably due to the dilution of blood by hypervolemia, or suppression of erythropoiesis (release of erythropoietin) because the renal cortex would be exposed to the increased oxygen content in the blood during DRI of HbV as oxygen carriers. The slight hypertension 1 day after DRI would be related to the blood hyperviscosity or hypervolemia due to the presence of HbV. However, the Hct and RBC counts returned to levels similar to those of the saline group 14 days after DRI. The time course of the HbV concentration in plasma indicates that the rate of HbV clearance gradually increased and the concentration reached a plateau, probably due to the nonspecific phagocytic activation of the RES that was clarified previously by a carbon clearance measurement (Sakai et al., 2001). The accelerated liposome clearance of the second infusion was well characterized (Claassen et al., 1988; Laverman et al., 2001); however, its mechanism, antibody formation or complement activation is controversial (Dams et al., 2000; Ishida et al., 2003).

In our previous report, the bolus HbV infusion (20 ml/kg) resulted in significant splenomegaly (about 100% increase) and hepatomegaly (13%) (Sakai et al., 2004b). In the present DRI study, splenomegaly was enhanced (190%), whereas hepatomegaly was similar (14%), indicating that the spleen had a larger capacity for HbV clearance. A large amount of HbV accumulated in the red pulp zone of the spleen and in Kupffer cells of the liver; however, 14 days later it disappeared and the splenohepatomegaly completely subsided. The spleen and the liver showed significant hemosiderin deposition; however, the enzyme concentrations that reflect the liver function did not show any abnormal values.

One day after DRI, the mesangial cells in the renal glomerulus seemed to entrap HbV in their intracellular spaces, and the same portion was stained with Berlin blue 1 and 14 days after DRI. In our previous report on the bolus HbV infusion, there was no abnormality in the kidneys (Sakai et al., 2004b). According to Rudolph et al. (1995), liposome-encapsulated Hb without PEG-modification aggregated in the plasma and showed a slight accumulation in the kidneys. Even though our PEG-modified HbV does not induce intervesicular aggregation, HbV would tend to be aggregated during the longer circulation time due to the DRI. No abnormal value was noted for UA, BUN, and CRE, although urinalysis showed a slight increase in protein levels.

Lipase activity, but not that of amylase, significantly in-

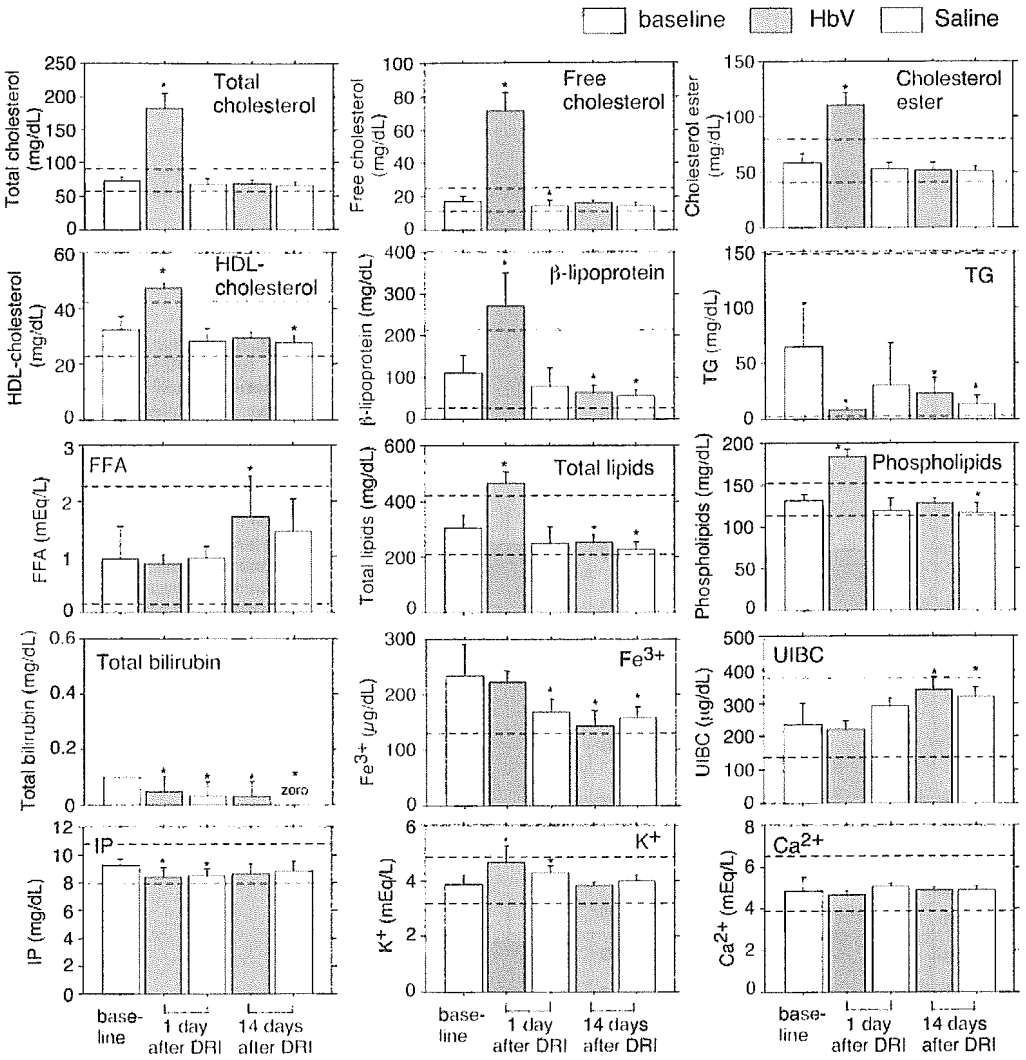

Fig. 7. Plasma clinical chemistry tests reflecting the metabolism of lipids and Hb and electrolytes 1 or 14 days after DRI of HbV or saline. The values are mean ± S.D. *, significantly different versus the baseline group. The dotted lines indicate the levels of 2× S.D. TG, triglyceride; FFA, free fatty acid; UIBC, unsaturated iron-binding capacity; IP, inorganic phosphate.

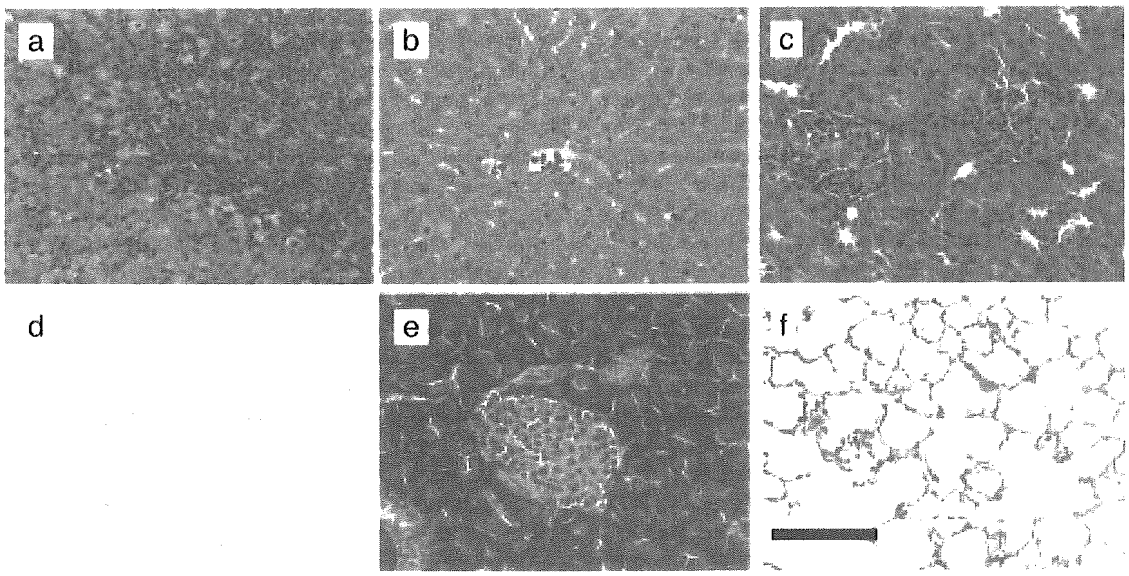

Fig. 8. Histology of spleen (a), liver (b), kidneys (c), heart (d), pancreas (e), and lungs (f) 1 day after DRI of HbV. A significant amount of HbV was accumulated in the red pulp zone of the spleen. The invasion of a significant number of Kupffer cells with HbV was seen in the liver. In the kidneys, the mesangial cells in the renal glomeruli seemed to entrap HbV. The myocardium showed slight staining with Berlin blue. No significant pathological changes are noted in the pancreas and lungs. Scale bar, 100 μm. Hematoxylin and eosin stains (a, b, c, e, and f) and Berlin blue stain (d).

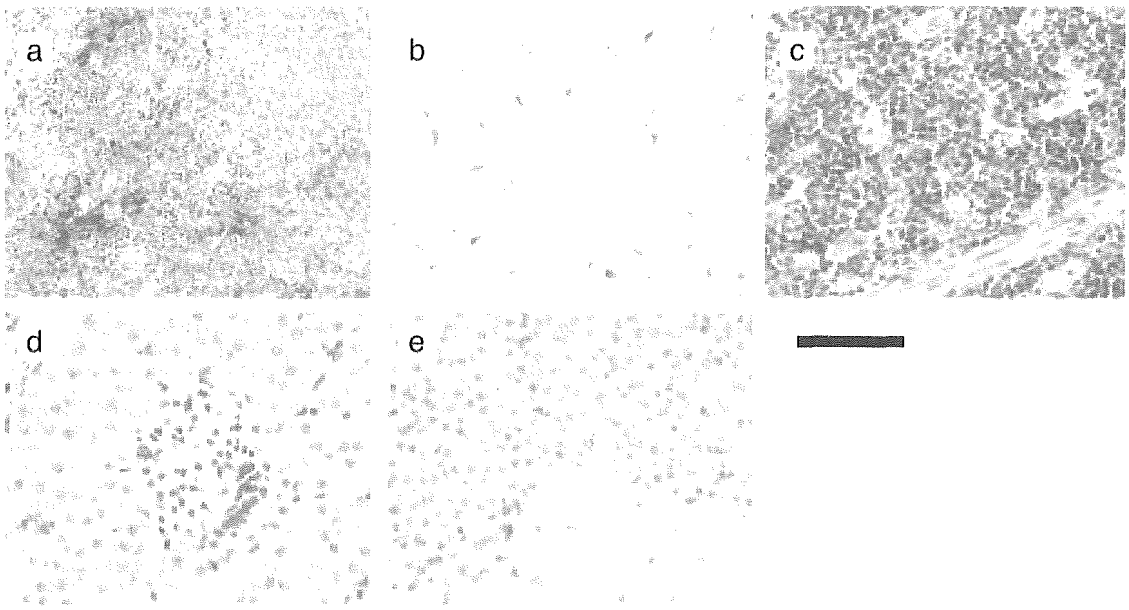

Fig. 9. Histology of spleen (a), liver (b), bone marrow (c), kidneys (d), and adrenal gland (e) 14 days after DRI. Berlin blue staining was performed to examine the presence of hemosiderin. Scale bar, 100 μm.

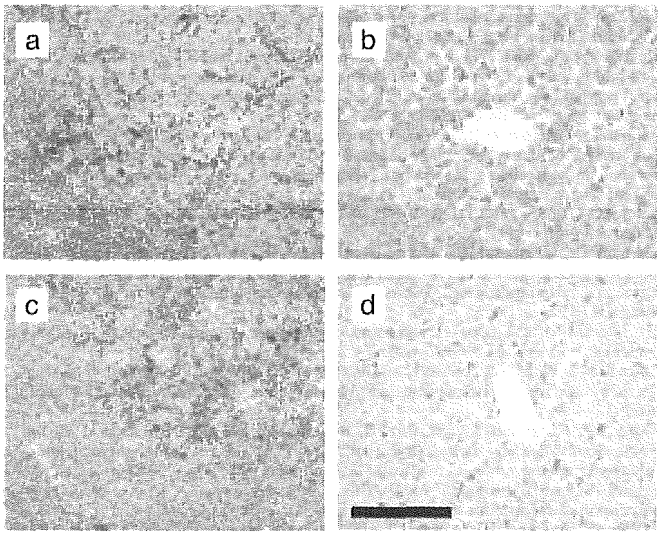

Fig. 10. Double immunohistochemical staining for HO-1 and human Hb in HbV in the rat spleen (a and c) and liver (b and d), 1 (a and b) and 14 days (c and d) after DRI of HbV. The tissues were stained with anti-rat HO-1 monoclonal antibody (GTS-3). The brown-colored portions (a, c, and d) indicate the presence of HO-1, and the pink or gray-beige areas (a and b) indicate the presence of a large amount of HbV. Scale bar, 100 μm.

creased in the HbV group, whereas there was no histopathological abnormality in the pancreas. A similar tendency was observed after the bolus HbV infusion (20 ml/kg) (Sakai et al., 2004b). This level of increment was significantly smaller than the value for the Wistar rats with acute necrotizing pancreatitis that increased the lipase activity from 10 to 475 to 5430 IU/l (Hofbauer et al., 1996). One possible reason for the moderate and specific increase in lipase activity would be related to the enzyme induction in the pancreas by the presence of a large amount of lipids from the liposomes (Stueckllin-Utsch et al., 2002), because pancreatic lipase hydrolyzes not only triglyceride but also phosphatidylcholine (Rowland and Woodley, 1980). However, the mechanism is not clear, and the pancreatic function should be carefully monitored in the ongoing safety studies.

The plasma lipid components significantly increased after the DRI of HbV. They should be derived from HbV because it contains a large amount of cholesterol and DPPC, and they would be liberated after the HbV particles are captured and degraded in the RES. It is reported that once liposome is captured in the Kupffer cells, the diacylphosphatidylcholine is metabolized and is reused as a cell membrane component or excreted in the bile (Dijkstra et al., 1985; Verkade et al., 1991). Cholesterol is finally catabolized as bile acids in the parenchymal hepatocytes. There should be no direct contact of HbV and the hepatocytes because HbV (diameter, 250 nm) cannot diffuse across the fenestrated endothelium into the space of Disse (Goda et al., 1998). Cholesterol of the vesicles should reappear in the blood mainly as lipoprotein cholesterol after entrapment in the Kupffer cells and should then be excreted in the bile after entrapment of the lipoprotein cholesterol by the hepatocytes (Kuipers et al., 1986). Judging from the results showing that the increases in the plasma lipid components were transient, the lipid components of HbV would gradually be redistributed, metabolized, and excreted in the same manner within 14 days after DRI. However, the details have to be confirmed by the biodistribution of the radiolabeled components.

In spite of the massive HbV infusions, the plasma bilirubin and iron levels did not increase. Urinalysis also showed no increase in the urobilinogen and bilirubin. The anti-human Hb antibody staining detected temporal distributions of HbV in the spleen and liver. The excess amount of heme from Hb in HbV should be metabolized by the inducible form of HO-1 in the spleen macrophages and the liver Kupffer cells, as shown in Fig. 10 (Braggins et al., 1986; Goda et al., 1998). Bilirubin should be excreted in the bile as a normal physiological pathway even during the massive doses of HbV. No increase in the plasma bilirubin level indicated that there was no obstruction or stasis of bile in the biliary tree and that the heme-degrading capacity of the RES did not surpass the ability to eliminate

bilirubin. Berlin blue staining revealed the presence of hemosiderin in the liver, spleen, kidneys, adrenal gland, and bone marrow 14 days after DRI and also in the myocardium 1 day after DRI. Both ferritin and hemosiderein store and release iron molecules, and they are anticipated to induce hydroxyl radical production and succeeding lipid peroxidation. However, iron release from hemosiderin is substantially less than that from ferritin, thus iron molecules in hemosiderin are relatively inert (O'Connell et al., 1989). Multiple blood transfusions often induce hemosiderosis in many organs. Accordingly, Hb encapsulation in the phospholipid vesicles would guarantee the smooth metabolic route of HbV that is similar to the well characterized metabolic route of senescent RBCs in the liver Kupffer cells and spleen macrophages (Bennett and Kay, 1981; Hirano et al., 2001). This would be a great advantage over molecular Hb that incurs not only filtration across the fenestrated endothelium of the glomerular capillary in the kidneys resulting in shorter circulation time and renal failure but also extravasation from the sinusoidal caliber in the liver, causing cancellation of the CO-mediated fail-safe mechanism for conserving sinusoidal patency and bile formation (Kyokane et al., 2001).

In conclusion, all the rats tolerated the DRI of HbV with no deteriorative signs of the organ functions. The phospholipid vesicles for Hb encapsulation would be beneficial for heme detoxification through their preferential delivery to the RES, a physiological compartment for degradation of not only foreign materials but also the senescent RBCs. However, it has to be considered that in humans the circulation time of HbV and its degradation rate in the RES would be different compared with those in rats, because the circulation time of stealth liposomes and the life span of RBCs are different between rodents and humans (Landaw, 1988; Gabizon et al., 2003). A shock condition may also influence on the RES function.

Our results would provide important information not only for the ongoing safety studies of HbV but also for the overall research on liposomal drugs, because this study is the first attempt to infuse repetitively such a large amount of phospholipid vesicles.

Acknowledgments

We acknowledge researchers in the School of Medicine, Keio University; H. Abe, T. Yamaguchi, and S. Kurasaki (Department of Pathology) for excellent histopathological techniques; and Dr. Y. Izumi, Dr. M. Watanabe, and T. Ohba (Department of Surgery) and Dr. M. Kajimura (Department of Biochemistry) for discussions on the experimental procedures.

References

Bennett GD and Kay MM (1981) Homeostatic removal of senescent murine erythrocytes by splenic macrophages. *Exp Hematol* **9**:297–307.

Biro GP and Greenburg AG (1999) Safety toxicology evaluation of o-raffinose cross linked hemoglobin solution by daily repeated infusions in rats and dogs (Abstract). *Crit Care Med* **27 (Suppl)**:479.

Braggins PE, Trakshel GM, Kutty RK, and Maines MD (1986) Characterization of two heme oxygenase isoforms in rat spleen: comparison with the hematin-induced and constitutive isoforms of the liver. *Biochem Biophys Res Commun* **141**:528–533.

Chang TM, Lister C, Nishiya, and Varma R (1992) Immunological effects of hemoglobin, encapsulated hemoglobin, polyhemoglobin and conjugated hemoglobin using different immunization schedules. *Biomater Artif Cells Immobil Biotechnol* **20**:611–618.

Charrois GJR and Allen TM (2003) Multiple injection of pegylated liposomal doxorubicin: pharmacokinetics and therapeutic activity. *J Pharmacol Exp Ther* **306**: 1058–1067.

Claassen E, Westerhof Y, Versluis B, Kors N, Schellekens M, and van Rooijen N (1988) Effect of chronic injection of sphingomyelin-containing liposomes on lymphoid and non-lymphoid cells in the spleen. Transient suppression of marginal zone macrophages. *Br J Exp Pathol* **69**:865–875.

Dams ETM, Laverman P, Oyen WJG, Storm G, Scherphof GL, van der Meer JWM, Corsten FHM, and Boerman OC (2000) Accelerated blood clearance and altered biodistribution of repeated injections of sterically stabilized liposomes. *J Pharmacol Exp Ther* **292**:1071–1079.

Dijkstra J, van Galen M, Regts D, and Scherphof G (1985) Uptake and processing of liposomal phospholipids by Kuppfer cells in vitro. *Eur J Biochem* **148**:391–397.

Djordjevich L, Mayoral J, Miller IF, and Ivankovich AD (1987) Cardiorespiratory effects of exchanging transfusions with synthetic erythrocytes in rats. *Crit Care Med* **15**:318–323.

Fielding RM, Moon-Mcdermott L, Lewis RO, and Horner MJ (1999) Pharmacokinetics and urinary excretion of amikacin in low-clearance unilamellar liposomes after a single or repeated intravenous administration in the rhesus monkey. *Antimicrob Agents Chemother* **43**:503–509.

Gabizon A, Shmeeda H, and Barenholz Y (2003) Pharmacokinetics of pegylated liposomal Doxorubicin: review of animal and human studies. *Clin Pharmacokinet* **42**:419–436.

Goda N, Suzuki K, Naito S, Takeoka S, Tsuchida E, Ishimura Y, Tamatani T, and Suematsu M (1998) Distribution of heme oxygenase isoform in rat liver: topographic basis for carbon monoxide-mediated microvascular relaxation. *J Clin Investig* **101**:604–612.

Hamilton RG, Kelly N, Gawryl MS, and Rentko VT (2001) Absence of immunopathology associated with repeated IV administration of bovine Hb-based oxygen carrier in dogs. *Transfusion* **41**:219–225.

Hirano K, Kobayashi T, Watanabe T, Yamamoto T, Hasegawa G, Hatakeyama K, Suematsu M, and Naito M (2001) Role of heme oxygenase-1 and Kupffer cells in the production of bilirubin in the rat liver. *Arch Histol Cytol* **64**:169–178.

Hofbauer B, Friess H, Weber A, Baczako, Kisling P, Schilling M, Uhl W, Dervenis C, and Buchler MW (1996) Hyperlipaemia intensifies the course of acute oedematous and acute necrotising pancreatitis in the rat. *Gut* **38**:753–758.

Ishida T, Maeda R, Ichihara M, Irimura K, and Kiwada H (2003) Accelerated clearance of PEGylated liposomes in rats after repeated infusion. *J Controlled Release* **88**:35–42.

Izumi Y, Sakai H, Hamada K, Takeoka S, Yamahata T, Kato R, Nishide H, Tsuchida E, and Kobayashi K (1997) Physiologic responses to exchange transfusion with hemoglobin vesicles as an artificial oxygen carrier in anesthetized rats: changes in mean arterial pressure and renal cortical tissue oxygen tension. *Crit Care Med* **24**:1869–1873.

Kuipers F, Spanjer HH, Havinga R, Scherphof GL, and Vonk RJ (1986) Lipoproteins and liposomes as in vivo cholesterol vehicles in the rat: preferential use of cholesterol carried by small unilamellar liposomes for the formation of muricholic acids. *Biochim Biophys Acta* **876**:559–566.

Kyokane T, Norimuzu S, Taniai H, Yamaguchi T, Takeoka S, Tsuchida E, Naito M, Nimura Y, Ishimura Y, and Suematsu M (2001) Carbon monoxide from heme catabolism protects against hepatobiliary dysfunction in endotoxin-treated rat liver. *Gastroenterology* **120**:1227–1240.

Landaw SA (1988) Factors that accelerate or retard red blood cell senescence. *Blood Cells* **14**:47–59.

Laverman P, Carstens MG, Boerman OC, Dams ETM, Oyen WJG, Rooijen NV, Corstens FHM, and Storm G (2001) Factors affecting the accelerated blood clearance of polyethylene glycol-liposomes on repeated injection. *J Pharmacol Exp Ther* **298**:607–612.

Lian T and Ho RJY (2001) Trends and developments in liposome drug delivery systems. *J Pharm Sci* **90**:667–680.

O'Connell MJ, Ward RJ, Baum H, and Peters TJ (1989) Iron release from haemosiderin and ferritin by therapeutic and physiological chelators. *Biochem J* **260**:903–907.

Phillips WT, Klipper RW, Awasthi VD, Rudolph AS, Cliff R, Kwasiborski V, and Goins BA (1999) Polyethylene glycol-modified liposome-encapsulated hemoglobin: a long circulating red cell substitute. *J Pharmacol Exp Ther* **288**:665–670.

Rowland RN and Woodley JF (1980) The stability of liposomes in vivo to pH, bile salts and pancreatic lipase. *Biochim Biophys Acta* **620**:400–409.

Rudolph AS, Spielberg H, Spargo BJ, and Kossovsky N (1995) Histopathologic study following administration of liposome-encapsulated hemoglobin in the normovolemic rat. *J Biomed Mater Res* **29**:189–196.

Sakai H, Hara H, Yuasa M, Tsai AG, Takeoka S, Tsuchida E, and Intaglietta M (2000a) Molecular dimensions of Hb-based O_2 carriers determine constriction of resistance arteries and hypertension in conscious hamster model. *Am J Physiol* **279**:H908–H915.

Sakai H, Hisamoto S, Fukutomi I, Sou K, Takeoka S, and Tsuchida E (2004a) Detection of lipopolysaccharide in hemoglobin-vesicles by *Limulus* amebocyte lysate test with kinetic-turbidimetric gel clotting analysis and pretreatment with a surfactant. *J Pharm Sci* **93**:310–321.

Sakai H, Horinouchi H, Masada Y, Takeoka S, Kobayashi K, and Tsuchida E (2004b) Metabolism of hemoglobin-vesicles (artificial oxygen carriers) and their influence on organ functions in a rat model. *Biomaterials* **25**:4317–4325.

Sakai H, Horinouchi H, Tomiyama K, Ikeda E, Takeoka S, Kobayashi K, and Tsuchida E (2001) Hemoglobin-vesicles as oxygen carriers: influence on phagocytic activity and histopathological changes in metabolism. *Am J Pathol* **159**:1079–1088.

Sakai H, Masada Y, Horinouchi H, Yamamoto M, Ikeda E, Takeoka S, Kobayashi K, and Tsuchida E (2004c) Hemoglobin-vesicles suspended in recombinant human serum albumin for resuscitation from hemorrhagic shock in anesthetized rats. *Crit Care Med* **32**:539–545.

Sakai H, Tomiyama K, Masada Y, Takeoka S, Horinouchi H, Kobayashi K, and Tsuchida E (2003) Pretreatment of serum containing Hb-vesicles (oxygen carriers) to avoid their interference in laboratory tests. *Clin Chem Lab Med* **41**:222–231.

Sakai H, Tomiyama K, Sou K, Takeoka S, and Tsuchida E (2000b) Polyethyleneglycol-conjugation and deoxygenation enable long-term preservation of hemoglobin-vesicles as O_2 carriers in a liquid state. *Bioconjug Chem* **11**:425–432.

Sakai H, Tsai AG, Kerger H, Takeoka S, Tsuchida E, and Intaglietta M (1998)

Subcutaneous microvascular responses to hemodilution with a red cell substitute consisting of polyethyleneglycol-modified vesicles encapsulating hemoglobin. *J Biomed Mater Res* **40**:66–78.

Sou K, Endo T, Takeoka S, and Tsuchida E (2000) Poly(ethylene glycol)-modification of the phospholipid vesicles by using the spontaneous incorporation of poly(ethylene glycol)-lipid into the vesicles. *Bioconjug Chem* **11**:372–379.

Sou K, Naito Y, Endo T, Takeoka S, and Tsuchida E (2003) Effective encapsulation of proteins into size-controlled phospholipid vesicles using freeze-thawing and extrusion. *Biotechnol Prog* **19**:1547–1552.

Stuecklin-Utsch A, Hasan C, Bode U, and Fleischhack G (2002) Pancreatic toxicity after liposomal amphotericin B. *Mycoses* **45**:170–173.

Teicher BA, Ara G, Herbst R, Takeuchi H, Keyes S, and Northey D (1997) PEG-hemoglobin: effects on tumor oxygenation and response to chemotherapy. *In Vivo* **11**:301–311.

Verkade HJ, Derksen JT, Gerding A, Scherphof GL, Vonk RJ, and Kuipers F (1991) Differential hepatic processing and biliary secretion of head-group and acyl chains of liposomal phosphatidylcholines. *Biochem J* **275**:139–144.

Address correspondence to: Prof. Eishun Tsuchida, Advanced Research Institute for Science and Engineering, Waseda University, Tokyo 169-8555, Japan. E-mail: eishun@waseda.jp

0022-3565/05/3122-702-709$20.00
THE JOURNAL OF PHARMACOLOGY AND EXPERIMENTAL THERAPEUTICS
Copyright © 2005 by The American Society for Pharmacology and Experimental Therapeutics
JPET 312:702-709, 2005

Vol. 312, No. 2
74534/1187652
Printed in U.S.A.

Circulation Kinetics and Organ Distribution of Hb-Vesicles Developed as a Red Blood Cell Substitute

Keitaro Sou, Robert Klipper, Beth Goins, Eishun Tsuchida, and William T. Phillips

Advanced Research Institute for Science and Engineering, Waseda University, Tokyo, Japan (K.S., E.T.); and Department of Radiology, University of Texas Health Science Center at San Antonio, San Antonio, Texas (R.K., B.G., W.T.P.)

Received July 20, 2004; accepted September 30, 2004

ABSTRACT

Phospholipid vesicles encapsulating concentrated human hemoglobin (Hb-vesicles, HbV), also known as liposomes, have a membrane structure similar to that of red blood cells (RBCs). These vesicles circulate in the bloodstream as an oxygen carrier, and their circulatory half-life times ($t_{1/2}$) and biodistribution are fundamental characteristics required for representation of their efficacy and safety as a RBC substitute. Herein, we report the pharmacokinetics of HbV and empty vesicles (EV) that do not contain Hb, in rats and rabbits to evaluate the potential of HbV as a RBC substitute. The samples were labeled with technetium-99m and then intravenously infused into animals at 14 ml/kg to measure the kinetics of HbV elimination from blood and distribution to the organs. The $t_{1/2}$ values were 34.8 and 62.6 h for HbV and 29.3 and 57.3 h for EV in rats and rabbits, respectively. At 48 h after infusion, the liver, bone marrow, and spleen of both rats and rabbits had significant concentrations of HbV and EV, and the percentages of the infused dose in these three organs were closely correlated to the circulatory half-life times in elimination phase ($t_{1/2\beta}$). Furthermore, the milligrams of HbV per gram of tissue correlated well between rats and rabbits, suggesting that the balance between organ weight and body weight is a fundamental factor determining the pharmacokinetics of HbV. This factor could be used to estimate the biodistribution and the circulation time of HbV in humans, which is estimated to be equal to that in rabbit.

Hemoglobin (Hb) isolated and purified from red blood cells (RBCs) has been tested as a principal component of RBC substitutes for carrying oxygen. However, the plasma retention time of isolated Hb is particularly short (half-life of ~0.5–1.5 h) because of the dissociation of the Hb tetramer into the dimeric form, which is subsequently filtered by the kidney, and it is known that this dimeric form is nephrotoxic (Savitsky et al., 1978). The potential of phospholipid vesicles as effective carriers of proteins and other bioactive materials has previously been proposed, since the cellular structure of such vesicles can protect the entrapped material from degradation and improve the biodistribution of proteins and other bioactive materials (Gregoriadis and Neerunjun, 1974; Papahadjopoulos et al., 1991). Phospholipid vesicles encapsulating concentrated Hb (HbV) have been proposed as a promising candidate RBC substitute, because encapsulation of Hb within a lipid membrane decreases potential side effects and toxicity of Hb, thereby making vesicles more RBC-like (Djordjevich and Miller, 1980; Gaber and Farmer, 1984; Tsuchida, 1998). The study of the safety and efficacy of HbV formulations by our research group has led to the development of an HbV formulation as a promising candidate for introduction into clinical trials (Tsuchida, 1998; Sakai et al., 2000b, 2001, 2004b; Takeoka et al., 2002).

Determination of the circulation time (half-life) of vesicles has been an important research focus, especially in RBC substitute development, because prolonged oxygen delivery is a required property for an artificial oxygen carrier. There are many reports describing the pharmacokinetics of vesicles, especially in mice and rats; however, it is difficult to apply these published data to the quantitative simulation of a clinical application. This is because of the lack of understanding of the species dependence of relevant mechanisms and correlative factors related to the clearance kinetics of vesicles. Some reports suggest that the circulatory half-life of vesicles injected in small doses into small animals such as

This work was supported in part by project of Health Science Research Grants (Artificial Blood Project) from the Ministry of Health, Labor and Welfare, Japan. K.S. was an overseas Research fellow of the Society of Japanese Pharmacopoeia (2002).
Article, publication date, and citation information can be found at http://jpet.aspetjournals.org.
doi:10.1124/jpet.104.074534.

ABBREVIATIONS: RBC, red blood cell; HbV, hemoglobin vesicle(s); EV, empty vesicle(s); ^{99m}Tc, technetium-99m; PEG, polyethylene glycol; DPPC, 1,2-dipalmitoyl-*sn*-glycero-3-phosphocholine; DPEA, 1,5-dihexadecyl-L-glutamate-*N*-succinic acid; PEG-DSPE, 1,2-distearoyl-*sn*-glycero-3-phosphoethanolamine-*N*-[monomethoxy poly(ethylene glycol) (5000)]; PLP, pyridoxal-5′ phosphate; HMPAO, hexamethylpropyleneamine oxime; %ID, percentage of infused dose; MPS, mononuclear phagocyte system.